IEEE Access
Multidisciplinary | Rapid Review | Open Access Journal

Received 15 September 2023, accepted 10 October 2023, date of publication 19 October 2023, date of current version 30 October 2023.

Digital Object Identifier 10.1109/ACCESS.2023.3325960

SURVEY

Machine Learning Approaches for Segmentation of Cardiovascular Neurocristopathy Related Images

TALHA IQBAL[1], OSAMA SOLIMAN[2,3], SHERIF SULTAN[2,3], AND IHSAN ULLAH[1,4]

[1]Insight SFI Research Centre for Data Analytics, University of Galway, Galway, H91 TK33 Ireland
[2]CORRIB-CURAM-Vascular Group Collaborators, University of Galway, Galway, H91 TK33 Ireland
[3]Discipline of Cardiology, University of Galway, Galway, H91 TK33 Ireland
[4]School of Computer Science, University of Galway, Galway, H91 TK33 Ireland

Corresponding author: Ihsan Ullah (ihsan.ullah@universityofgalway.ie)

This research was conducted with the financial support of Science Foundation Ireland under Grant Agreement No SFI/12/RC/2289_P2 at the Insight SFI Research Centre for Data Analytics in the University of Galway.

ABSTRACT Cardiovascular neurocristopathy is associated with abnormal migration and development of neural crest cells, impacting the neural and the human cardiovascular system and leading to diseases such as cardiomyopathy, aortic disease, and aortic valve dysfunction. With advancements in biomedical imaging tools, efforts are made to understand the underlying causes of cardiovascular neurocristopathy and develop new diagnostic methods, especially using machine learning or specifically its sub-branch deep learning models. This article provides a systematic survey of the literature related to machine/deep learning-based segmentation of the diseases mentioned above in computer tomography (CT), magnetic resonance imaging (MRI), X-rays, and echocardiogram (Echos) images. The review identified gaps and provides future directions, such as the need for better interpretable and explainable AI models, addressing the lack of publicly available datasets, standardizing the result reporting procedure for better repeatability of the result, and the development of standard performance measurement metrics. The general conclusion suggests that there is a need for multimodalities, multimodel, high-quality data sets, and open-source disease-specific dataspaces that will help develop trustworthy deep learning models that could be implemented in imaging devices/tools and provide medical-grade segmented outputs that will augment and speed up clinician decision making.

INDEX TERMS Cardiovascular, neurocristopathy, segmentation, neural networks, machine learning, deep learning, imaging, automation.

I. INTRODUCTION

In recent times, clinical and therapeutic needs have been increasing. According to the World Health Organization (WHO) report published in 2020, cardiovascular disease (CVD) is the leading cause of death in the world, responsible for 16% (8.9 million) of worldwide deaths.[1] As cardiovascular disease continues to be the leading cause of death worldwide,[2] the need for a timely and accurate diagnosis has never been more important [1]. Neurocristopathy is a pathological disorder that occurs due to an abnormal development and/or migration of neural crest cells, during embryonic development [2]. During embryonic development, the migration, abnormal specification, differentiation, or death of neural crest cells results in different neurocristopathies. Various diseases such as thyroid, skin pigments, heart and craniofacial abnormalities, tumors, and digestive tract dysfunction are some examples of neurocristopathies [3]. In this paper, we will focus on some cardiovascular neurocristopathy , such as cardiomyopathies, stroke, bicuspid aortic valve diseases and aortic vessel diseases.

Cardiovascular neurocristopathy is a genetic disorder that affects the development of the human cardiovascular system [4]. The formation of many different organs and tissues, including the heart and blood vessels, is dependent

The associate editor coordinating the review of this manuscript and approving it for publication was Derek Abbott.

[1]https://www.who.int/news-room/fact-sheets/detail/the-top-10-causes-of-death

[2]https://www.cdc.gov/globalhealth/healthprotection/ncd/cardiovascular-diseases.html

on the controlled migration and differentiation of neural crest cells [5]. Cardiovascular neurocristopathy occurs when gene mutations cause abnormal deaths of neural crest cells and reduce the performance of tissues/organs (for example, the heart) [6].

The aorta is the largest blood vessel and is responsible for oxygen circulation within the body [7]. Figure 1 shows the anatomy of the aorta and its branches.[3] From the figure we can see that the aorta gives rise to several branches, including:

1) Ascending Aorta: This portion of the aorta carries blood upward and then curves to form the aortic arch.
2) Aortic Arch: The aortic arch is a curved segment of the aorta that gives rise to several major arteries that supply the head, neck, and upper extremities. These branches include the brachiocephalic artery (which further divides into the right subclavian and right common carotid arteries), the left common carotid artery, and the left subclavian artery.
3) Descending Aorta: The aorta continues downward as the descending aorta (region below the left subclavian) and is divided into the thoracic aorta (supplying the chest area) and the abdominal aorta (supplying the abdominal region and lower extremities).

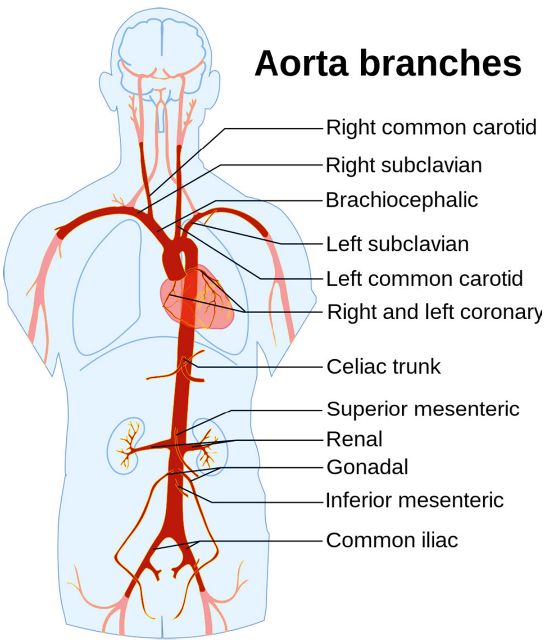

FIGURE 1. **Aorta and its branches anatomy (image source: Wikimedia Commons, license: CC BY-SA 3.0).**

Efforts are being made to better understand the underlying causes of cardiovascular neurocristopathy and develop new approaches to the diagnosis, treatment, and prevention of such disorders, especially focusing on machine learning and deep learning models [8], [9], [10]. Untreated cardiovascular neurocristopathy conditions have severe effects on human health and can cause cardiomyopathy, stroke, aorta, and aortic valve dysfunction diseases [11]. Each of the mentioned conditions is defined as follows.

Cardiomyopathy is a disease that affects the shape, thickness, and/or size of the heart muscle [12]. Cardiomyopathy can be divided into four subtypes [13], which are itemized below:

1) *Dilated cardiomyopathy*: where the heart muscle wall becomes thinner and stretched.
2) *Hypertrophic cardiomyopathy*: where the heart muscle wall thickens.
3) *Restrictive cardiomyopathy*: A set of changes occurs in the heart that limits its ability to expand or contract to pump blood into/out of the heart.
4) *Arrhythmogenic right Ventricular Cardiomyopathy (ARVC)*: In this condition, fatty fibrous tissue replaces normal heart tissue, causing abnormal heart rhythms.

Stroke may occur due to a blood clot reaching the brain as a result of a tear in the wall of the large blood vessel (in the neck), which is known as a dissection of the cervical artery [14]. **Bicuspid aortic valve diseases** could be classified into two classes:

1) *Bicuspid aortic disease with aortopathy*: where an aortic valve contains only two cusps (or flaps) instead of three with a weakened aorta.
2) *Bicuspid aortic disease without aortopathy*: an aortic valve that contains only two cusps (or flaps) instead of three without a weakened aorta.

Whereas, symptoms of the **aortic vessel disease** include:

1) *Aortic dissection*: where there is a tear in the inner layer of the aorta.
2) *Aortic aneurysms*: where a balloon-shaped bulge is formed in the aorta.
3) *Aortic hematoma*: where the pool of clotted blood forms an organ, tissue, or body space.

Figure 2 illustrates the anatomy of different cardiovascular neurocristopathy diseases.[4]

The current literature presents the use of different imaging and sensory techniques as well as health records for the diagnosis of these diseases [4], [15], [16], [17]. In imaging, magnetic resonance imaging (MRI) and computerized tomography (CT) are the most widely used modalities. The echocardiogram (Echo) is used for the assessment of associated cardiac abnormalities while X-rays are the most widely used for screening. The electrocardiogram (ECG) and the photoplythesmogram (PPG) are included in the sensory methods. Some studies use electronic health records (EHR) to collect data or identify those already diagnosed with the disease. Diagnosis of diseases such as CV neurocristopathies

[3] Mikael Häggström, based on work by Edoarado [CC BY-SA 3.0], via Wikimedia Commons (Aorta. (2023, 12 May). In Wikipedia. https://en.wikipedia.org/wiki/Aorta)

[4] 2a: work by BruceBlaus [CC BY-SA 4.0], via Wikimedia Commons (Thoracic Aortic Aneurysm. (2023, May 12); 2b: work by Npatchett [CC BY-SA 4.0], via Wikimedia Commons (Aortic_dissection_types. (2023, May 12); 2b: work by Drj [CC BY-SA 3.0], via Wikimedia Commons (Aortic_valve_pathology_CardioNetworks_ECHOpedia). (2023, 12 May).

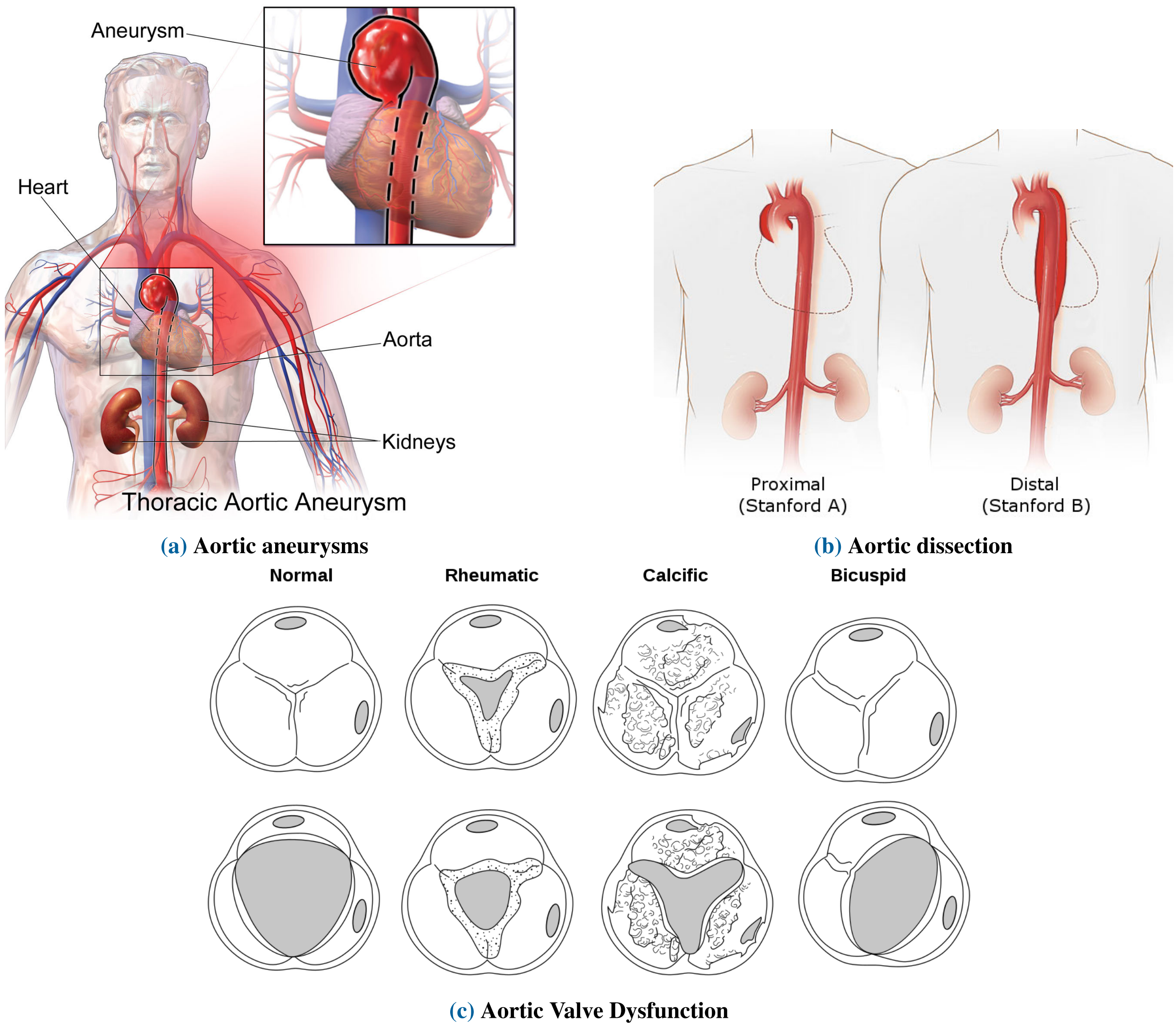

FIGURE 2. Anatomy of different cardiovascular neurocristopathy diseases. (a) Aortic aneurysms: where a balloon-shaped bulge is formed in the aorta. (b) Aortic dissection: where there is a tear in the inner layer of the aorta. (c) Bicuspid aortic disease: where an aortic valve contains only two cusps (or flaps) instead of three. (image source: Wikimedia Commons, license: CC BY-SA 4.0, 3.0 and 4.0, respectively).

require often history taking, imaging, and bio-markers and it requires specific criteria to establish the diagnosis. These are called diagnostic criteria.

This paper focuses on reviewing the available literature on the segmentation of aforementioned diseases where imaging data is used as input for analysis.

A. DIFFERENTIATING/COMPARING MODALITIES FROM A COMPUTER SCIENCE PERSPECTIVE

From the perspective of computer science, each of the imagining modalities is different in terms of sensors providing different information about the heart.

1) *X-ray*: An X-ray is a black-and-white image that captures the outline of the heart and the major blood vessels. X-rays are useful for the detection of large structural abnormalities but do not provide details on heart function [18]. X-rays are the building block of the computer tomography image and are usually not used alone for the detection and segmentation of cardiovascular diseases [19].
2) *Computer Tomography (CT)*: Computer tomography is a 3D image that captures details of the size, shape, and function of the heart, as well as any narrowing or blockage of the arteries [20]. CT images provide accurate information for the diagnosis, segmentation, and monitoring of cardiovascular diseases. However, it uses ionizing radiation (X-rays), which is harmful in high doses and therefore not suitable for certain vulnerable patients [21].
3) *Magnetic Resonance Imaging (MRI)*: Magnetic resonance imaging is a high-resolution image captured using a magnetic field, rather than radiation, and a sophisticated machine to capture information about the heart and arteries [22]. Magnetic resonance imaging

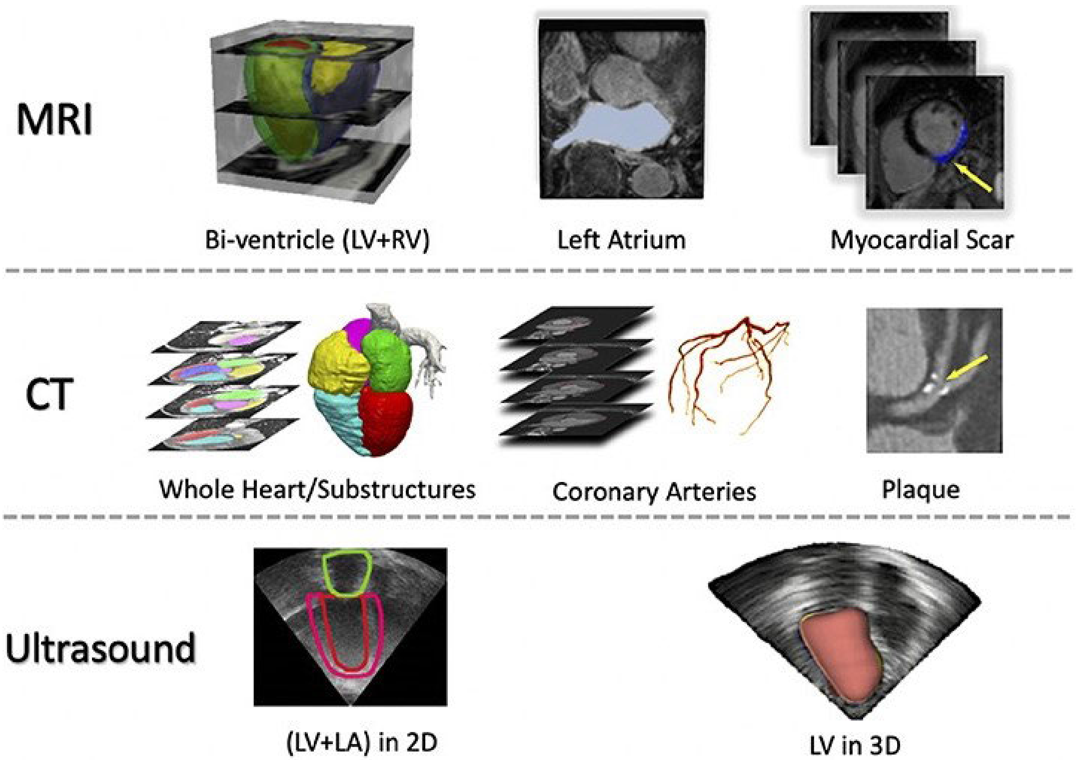

FIGURE 3. Overview of image segmentation tasks for different imaging modalities. Adopted from [8].

provides detailed images of the structure and functionality of the heart, including areas of narrowing, blockage, and leakage in the heart, as well as in the arteries. However, MRI scans are time-consuming, expensive and not suitable for patients who are claustrophobic or who have implants [23].

4) *Echocardiography (Echo)*: An echocardiogram captures sound waves that bounce off the heart and its blood vessels to provide information about its structure and function, including how the heart pumps blood and the extent of any narrowing or blockages of the arteries [24]. Echoes are inexpensive, noninvasive, and can be performed quickly and at the bedside. The images produced through this method are less detailed and low-resolution compared to CT and MRI, therefore, they are only used if continuous monitoring of vulnerable patients is required [25].

The image quality and information within the images obtained through each modality are different and have a significant impact on the development of the segmentation model. The image quality directly affects the training and validation accuracy of segmentation algorithms in identifying and delineating anatomical structures. Higher image quality enhances precision while lower-quality image introduces challenges and errors. Furthermore, the information contained within the images also varies across modalities. Some modalities (such as CT and MRI) provide more detailed anatomical information while some modalities (X-ray and Echos) provide only functional/physiological information.

Understanding the different imaging modalities from the point of view of a computer scientist is essential for the development of better diagnostic tools and tools that could be utilized to efficiently analyze and interpret medical images. Computer scientists must consider the above-mentioned factors to select appropriate imaging modalities and develop robust segmentation models that ensure optimal performance and reliable results.

B. CHALLENGES

The traditional imaging techniques/tools have significant challenges, which limit the clinical and prognostic ability of these tools [26], [27], [28]. Some of these challenges are as follows:

1) Inter- and Intra-observer variability: Interobserver variability refers to variability in the results when different doctors/physicians interpret the same image, whereas intraobserver variability refers to variability in the results when the same doctor/physician interprets the same image multiple times. In other words, the ground-truth information available for training will not be the same or accurate.
2) Delayed reporting on image results: Time-consuming exams can delay the diagnosis and treatment of patients. In some cases, they may have to wait hours and/or days to receive results, which leads to anxiety and uncertainty.
3) Suboptimal image quality: The low-quality images limit the clinical validation of cardiovascular images.

It is difficult to see certain areas of the heart in low-quality images, leading to misdiagnoses or inaccurate assessments of the severity of the disease. The sub-optimal image quality also hinders the development of a segmentation model due to limited visual information for training.

4) Operator fatigue: Performing multiple exams and long shifts in a day can be physically and mentally tiring, resulting in possible errors or/and inaccurate results.
5) Radiation exposure and contrast agents: Repeated exposure to ionizing radiation over time and the use of contrast agents to enhance the resolution of a certain structure could increase the chances of developing cancer in certain patients. Furthermore, the contrast levels of the images are also varied for different devices/machines. Thus, a model trained on a certain level of contrast images might not work on images taken through another machine, due to the contrast difference.
6) Inter-vendor variability: Inter-vendor variability in certain imaging parameters such as myocardial strain imaging and perfusion images might limit the generalizability of ML algorithms across all vendors and scanners.

With continuous technological advancement in the field of cardiovascular imaging, researchers are motivated to develop different analysis tools to overcome the challenges/limitations mentioned above [29], [30], [31], [32], [33], [34], [35]. This will help doctors/clinicians diagnose the disease accurately and design better treatment plans for their patients [36], [37], [38]. The application of artificial intelligence (AI), especially machine learning (ML) and deep learning (DL), in the field of medical imaging has been growing rapidly in recent years [39], [40]. Traditional ML algorithms are fed manually hand-crafted features, while DL algorithms automatically learn the same features for analysis [36].

This work is designed to review the available literature on the segmentation of the aforementioned diseases using imaging data with the help of ML and DL methods. The review covers different aspects of diagnosis using different imaging techniques and preventive care that no other single review covers. Table 1 provides a comparison of the proposed review with other recently published review articles.

The rest of the review article is organized as follows: Section II describes the search terms, the inclusion criteria, and the PRISMA flow chart. Section III provides a detailed review of the available literature on the different methodologies used for each disease and the advantages/limitations of each modality. It also discusses the clinical interpretation of the data and different ML / DL methods used for the segmentation of the aforementioned diseases. Section IV illustrates the findings and shortcomings learned from the literature review, while conclusions and future directions are provided in Section V.

II. SEARCH METHODOLOGY

This review is in accordance with the PRISMA guidelines [45], a preferred reporting process for systematic reviews and meta-analyses, illustrated in Figure 4. The literature searches were performed on the following platform:

- PubMed, Google Scholar, IEEE Xplore Digital Library, Elsevier, ScienceDirect, and Wiley online library.

The search terms were the combination of two primary terms (machine learning, deep learning, segmentation) and a maximum of one secondary term (Dilated cardiomyopathy, Hypertrophic cardiomyopathy, Restrictive cardiomyopathy, Arrhythmogenic right Ventricular Cardiomyopathy, aortic dissection, aortic aneurysms, aortic hematoma, bicuspid aortic valve disease with aortopathy, bicuspid aortic valve disease without aortopathy and cervical artery dissection).

Initially, 750 studies were identified, including both journal and conference publications. After reading the title and abstract, 100 articles were selected. Studies excluded after full-text evaluation included nonhuman studies, that had insufficient data or modality used other than MRI, CT, X-rays and/or Echo. A total of 48 articles were shortlisted for review after a full-text assessment.

III. DEEP LEARNING TOOLS FOR CARDIOVASCULAR NEUROCRISTOPATHY SEGMENTATION

Deep learning is a sub-branch of machine learning that utilizes structured and unstructured data to learn abstract representations [46]. These algorithms/models are advanced versions of neural networks with specialized layers and special structures for processing the neurons, allowing them to handle any data source and extract useful information [47]. Regarding cardiovascular neurocristopathy image processing, the convolutional layers with different numbers of kernels, play a critical role in the ability of algorithms to generate various feature maps that can help in identifying specific/hidden patterns such as edges, colour gradients, and shapes within the input image/video [48]. Subsequently, these learned patterns are used to perform segmentation analysis, that is, to detect specific objects or structures through pixel-level labelling [49]. Some common algorithms used for image segmentation include Convolutional Neural Networks (CNN) and their variants such as U-net, auto-encoders (AE), and generative adversarial networks (GAN) [50], [51].

The paper although mention both ML and DL, but for segmentation purpose, mainly the DL models are the focus because of their automatic nature of learning discriminative features and recent rapid increase in performance. Table 2 summarizes the performance metrics used in the reviewed studies along with the rationale and characteristics of each metric while the most frequently used DL and ML algorithms for medical imaging segmentation are tabulated in Table 3.

In terms of performance metrics (Table 2), the majority of reviewed studies used the dice score and the Hausdorff distance as primary performance measuring metrics along with a few other supporting metrics, such as sensitivity,

TABLE 1. Comparison of recent existing review articles with our review article.

S.NO.	Ref	Title	Year	Imaging modality				Modalities Definition	DL/ML Implementation	Challenges in tool	Cardiovascular Neurocristopathy diseases
				CT	MRI	X-rays	Echos				
1	[41]	Development and application of artificial intelligence in cardiac imaging	2020	✓	✓	x	x	x	x	x	cardiomyopathy
2	[8]	Deep Learning for Cardiac Image Segmentation: A Review	2020	✓	✓	x	✓	x	✓	x	cardiovascular structure and function (Aorta and Aortic Valve + whole heart)
3	[42]	Radiogenomics and Artificial Intelligence Approaches Applied to Cardiac Computed Tomography Angiography and Cardiac Magnetic Resonance for Precision Medicine in Coronary Heart Disease: A Systematic Review	2021	✓	✓	x	x	x	x	x	coronary heart disease (CHD)
4	[43]	Application of AI in cardiovascular multimodality imaging	2022	✓	✓	x	✓	x	x	x	cardiac valvular function and wall motion abnormalities
5	[44]	Artificial Intelligence Applications in Aortic Dissection Imaging	2022	✓	x	x	x	x	x	x	aortic dissection
6	**Our**	**Review on Machine and Deep Learning Approaches for Cardiovascular Neurocristopathy**	**2023**	✓	✓	✓	✓	✓	✓	✓	**cardiomyopathy (4 types), aortic dissection, aortic aneurysms, aortic hematoma, bicuspid aortic disease with aortopathy, bicuspid aortic disease without aortopathy and cervical artery dissection**

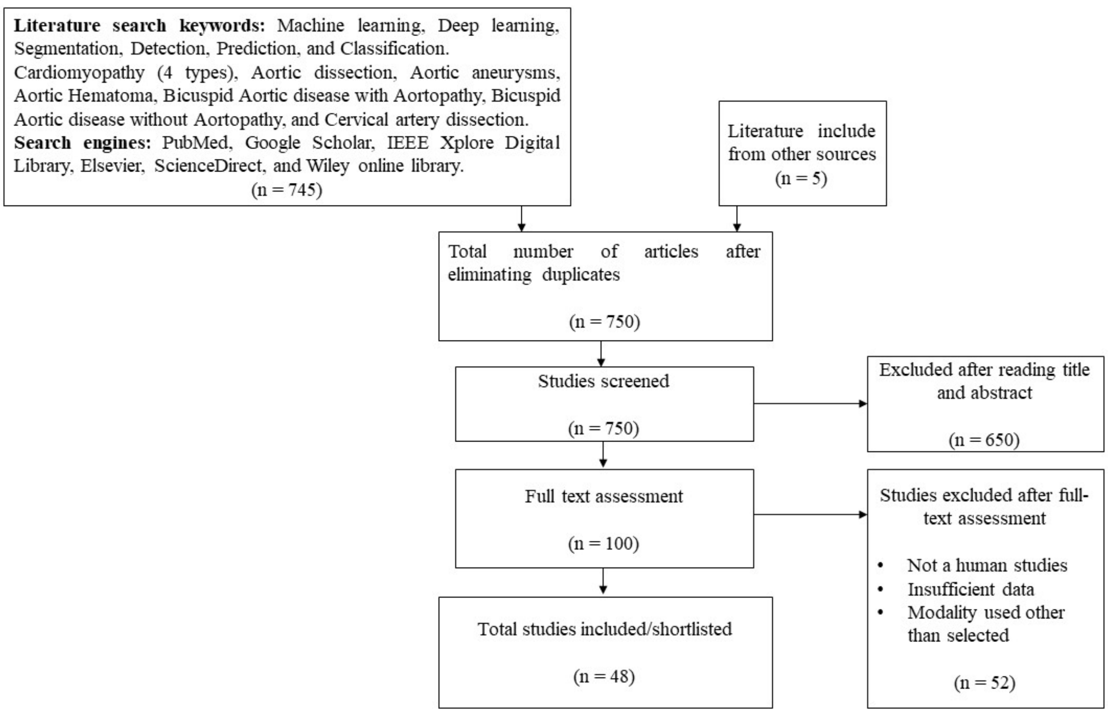

FIGURE 4. Adopted PRISMA guidelines and papers retrieved in this review.

specificity, Intersection-over-Union (IoU), correlation score, and average symmetrical surface distance to determine the efficacy of their segmentation model. These metrics are commonly used in the medical field as they provide valuable insights into different aspects of the segmentation model's performance. The Dice score and IoU evaluate the spatial overlap between ground truth and predicted segmentation, which is important for the delineation of the anatomical structure [52]. The Hausdorff Distance estimates the maximum deviation between ground truth and predicted segmentation and is useful in identifying segmentation outliers [53]. The Sensitivity and Specificity metrics help in assessing the model's ability to correctly identify positive and negative cases [54]. The Correlation Score measures the relationship between the ground truth and predicted segmentation, which can be informative for quantitative measurements [55]. Finally, the Average Symmetrical Surface Distance quantifies the average distance between ground truth and predicted segmentation providing boundary accuracy and smoothness of segmentation [56].

The table 3 summarizes the modality, performance metrics, sample size, data availability, and DL / ML algorithms implemented in 24 reviewed articles. One of the most significant challenges in segmenting and treating cardiovascular neurocristopathy disorders is the limited availability of open source publicly accessible data set on the disease, as evidenced by Table 3. Only one out of 24 studies (Guo et al. [57]) has provided the data set on which they worked. Furthermore, nine other studies ([58], [59], [60], [61], [62], [63], [64], [65], [66]) have mentioned that the data set could be provided to researchers on a reasonable request. All other remaining 18 studies (66.7%) have not noted the availability of their dataset.

As mentioned in I-A, CT and MRI are 3D imaging techniques that provide high-resolution, detailed, and sophisticated images, making them the more trustworthy modality for segmenting cardiovascular diseases. Some studies such as Asif et al. [63] and Qin et al. [67] used CT images for segmentation and compared their results with MRI data. Asif et al. performed segmentation on CT images and assessed segmentation accuracy using MRI as a reference standard collected from 84 patients (45 men and 32 women who underwent CT and MRI scans). The authors reported an AUC of 0.714 and a segmentation accuracy of 68.9% for males and 71.9% for female patient images. Qin et al. performed a semi-automated segmentation on CT and MRI data collected from 161 patients (2576 segments) with cardiomyopathy. They calculated 1514 myocardial fibrosis (MF) features and applied radiomics to the extracted features. The reported result showed the usefulness of radiomics in the segmentation and detection of MF using CT images (and compared to MRI). The authors reported that the AUC for the training and testing cohorts was 0.81 and 0.78 for the segment-based analysis, respectively.

Learning models for disease segmentation using medical images like CT scans, MRI, X-rays, and echocardiograms present several challenges due to the complexity and importance of the task. The following subsections summarise some of the challenges and potential solutions as well as provide review of different deep/ML algorithms used for cardiovascular neurocristopathy diseases with individual image modalities (CT, MRI, X-Rays and Echos) along with the performance metrics used for their evaluation, the sample size used, and open-access availability of the dataset.

TABLE 2. Performance metrics used in the medical domain for segmentation assessment.

Metric	Rationale	Features/Characteristics
Dice Score	Measures overlap between predicted and ground truth segmentation	- Ranges from 0 to 1, where 1 indicates perfect overlap and 0 indicates no overlap. - Useful for assessing spatial agreement between segmentations.
Hausdorff Distance	Captures maximum deviation between predicted and ground truth	- Represents the maximum distance between any point in one segmentation and its nearest point in the other. - Identifies outliers or extreme deviations in segmentation.
Sensitivity	Evaluates true positive rate (TPR)	- Measures the proportion of actual positive cases that are correctly identified by the model.
Specificity	Evaluates true negative rate (TNR)	- Measures the proportion of actual negative cases that are correctly identified by the model.
Intersection-over-Union	Measures the ratio of the intersection to the union of regions	- Ranges from 0 to 1, where 1 indicates perfect overlap and 0 indicates no overlap. - Provides a measure of segmentation accuracy and similarity.
Correlation Score	Assesses the correlation between predicted and ground truth	- Indicates the strength and direction of the linear relationship between the predicted and ground truth segmentation. - Useful for tasks involving quantitative measurements.
Average Symmetrical Surface Distance	Quantifies the average surface distance between predicted and ground truth	- Measures the average distance between corresponding points on the predicted and ground truth segmentations. - Provides insights into boundary accuracy and smoothness of segmentations.

A. CHALLENGES AND POTENTIAL SOLUTIONS IN IMAGE SEGMENTATION

This subsection outlines certain difficulties encountered when working with medical images and offers insights into potential solutions aimed at creating an AI-powered clinical-grade medical image segmentation device for early detection and prognosis applications. *Limited Data:* Annotated medical image datasets can be limited in size due to privacy concerns and the difficulty of obtaining expert annotations. To mitigate this challenge, data augmentation techniques can be employed to generate additional training samples from the existing data. Transfer learning, where models pre-trained on large datasets are fine-tuned on medical data, can also help when data is scarce. *Annotation Quality:* Annotations for medical images need to be highly accurate, and inconsistencies or errors in annotations can lead to model biases. To address this, expert radiologists should review and verify annotations to ensure accuracy. *Interpatient Variability:* Patients can have significant anatomical and pathological variations, making it challenging for models to generalize. To enhance model generalization, data augmentation techniques that simulate variations can be used. Domain adaptation methods can also be employed to adapt models to specific patient populations. *Interpretability:* Medical professionals often require models to provide interpretable results and explanations for their predictions. To meet this

TABLE 3. Frequently used DL and ML algorithms in the field of cardiovascular neurocristopathy.

S.No.	Algorithm		Ref	Year	Modality	Performance metrics	Sample Size	Dataset Open-access
1	**Deep Learning**	Artificial Neural Network (ANN)	[58]	2022	MRI/CMRI	Matthew's correlation coefficient (MCC), accuracy, sensitivity, specificity	167 patients and 84 control	On request
			[68]	2020	Echo	Sensitivity, specificity, PPV and NPV, F1-score, +ve and –ve likelihood ratio	146 patients and 58 control	No
2		U-net	[69]	2021	CT	Sensitivity, PPV, Dice score (DSC), volume overlap error (VOE), relative volume difference (VD), and average symmetric surface distance (ASSD)	72 patients	No
			[70]	2021	CT	Recall (sensitivity), precision (positive predictive value [PPV]), and false-positive volume (FPV).	2319 participants	No
			[59]	2022	MRI/CMRI	Dice similarity coefficients	68 patients and 27 control	On request
			[71]	2022	CT	Dice similarity coefficient; mean absolute error (MAE); intraclass correlation coefficient (ICC)	1715 participants	No
			[60]	2022	MRI	Matthew's correlation coefficient (MCC)	39688 participants	On request
			[61]	2022	CT	Dice coefficient (DC), normalized mean absolute error (NMAE), and RMSE	154 patients	On request
3		Convolutional Neural Network (CNN)	[72]	2022	Echo	AUC, sensitivity, specificity, PPV (Positive Predictive Value) and NPV	6825 patients	No
4		Extremely Randomized Tree	[73]	2022	MRI/CMRI	AUC, sensitivity, specificity	32 patients and 11 control	No
5		Multilayer Perceptron	[74]	2021	Echo	accuracy, sensitivity, and specificity	49 patients	No
6		DeeplabV3+	[75]	2021	MRI/CMRI	Sensitivity, specificity, accuracy, PPV, NPV, FPR, FNR and AUC	198 patients	No
7		Inception-ResnetV2 model	[76]	2021	MRI/CMRI	Sensitivity, specificity, accuracy, PPV, NPV, FPR, FNR and AUC	198 patients	No
8		SE-ResNext-50	[62]	2023	Echo	AUC	158 patients	On request
9		Deep Convolutional Neural Network (DCNN)	[66]	2021	Echo	AUC, PPV, NPV, sensitivity and specificity	99 patients	No
9		Deep Convolutional Neural Network (DCNN)	[63]	2021	Echo + CT	ROC AUC, Precision-recall curve and decision curve analysis + accuracy, sensitivity and specificity	300 patients	On request
10		ResNet-18	[77]	2022	X-Rays	Precision, recall, F1-score, accuracy and visual verification via grad-CAM	3331 patients	On request
11		Multi-residual Blocks	[64]	2022	Echo	PPV, NPV, sensitivity and specificity, AUC	157 patients	No
12		ENET	[69]	2021	CT	Sensitivity, PPV, Dice score (DSC), volume overlap error (VOE), relative volume difference (VD), and average symmetric surface distance (ASSD)	72 patients	No
13		ERFNet	[69]	2021	CT	Sensitivity, PPV, Dice score (DSC), volume overlap error (VOE), relative volume difference (VD), and average symmetric surface distance (ASSD)	72 patients	No
14		Residual Neural Network-18	[65]	2022	X-Rays	Accuracy, precision, recall, and F-1 score and Visual verification via grad-CAM	3331 patients	On request
15	**Traditional Machine Learning**	Random Forest (RF)	[67]	2021	CT + MRI/CMRI	AUC, accuracy, sensitivity, and specificity rates	161 patients	No
			[78]	2020	MRI/CMRI	Matthew's correlation coefficient (MCC), accuracy, sensitivity, specificity and AUC	64 patients	No
			[73]	2022	MRI/CMRI	AUC, sensitivity, specificity	32 patients and 11 control	No
			[66]	2021	Echo + CT	ROC AUC, Precision-recall curve and decision curve analysis + accuracy, sensitivity and specificity	300 patients	On request
			[74]	2021	Echo	Accuracy, sensitivity, and specificity	49 patients	No
			[79]	2022	Echo	AUC	13050 patients	No
16		Naive Bayes (NB)	[58]	2022	MRI/CMRI	Matthew's correlation coefficient (MCC), accuracy, sensitivity, specificity	167 patients and 84 control	On request
			[78]	2020	MRI/CMRI	Matthew's correlation coefficient (MCC), accuracy, sensitivity, specificity and AUC	64 patients	No
			[57]	2021	CTA	AUC, sensitivity, specificity, PPV and NPV	1344 patients	Yes
17		Support Vector Machine (SVM)	[58]	2022	MRI/CMRI	Matthew's correlation coefficient (MCC), accuracy, sensitivity, specificity	167 patients and 84 control	On request
			[78]	2020	MRI/CMRI	Matthew's correlation coefficient (MCC), accuracy, sensitivity, specificity and AUC	64 patients	No
			[66]	2021	Echo + CT	ROC AUC, Precision-recall curve and decision curve analysis + accuracy, sensitivity and specificity	300 patients	On request
18		Logistic Regression (LR)	[58]	2022	MRI/CMRI	Matthew's correlation coefficient (MCC), accuracy, sensitivity, specificity	167 patients and 84 control	On request
			[57]	2021	CT + MRI/CMRI	AUC, sensitivity, specificity, PPV and NPV	1344 patients	Yes
			[68]	2020	Echo	Sensitivity, specificity, PPV and NPV, F1-score, +ve and –ve likelihood ratio	146 patients and 58 control	No
19		Distance-weighted K-Nearest Neighbor	[80]	2020	Echo + MRI/CMRI	AUC, accuracy, sensitivity, and specificity rates	108 patients	No
20		Extreme Gradient Boost (XGBoost)	[57]	2021	CT + MRI/CMRI	AUC, sensitivity, specificity, PPV and NPV	1344 patients	Yes
21		Tree-based Pipeline Optimization Tool (TPOT)	[81]	2022	MRI/CMRI	AUC, F1-score, accuracy, Precision, sensitivity, and specificity rates	91 patients and 44 control	No
22		Least Absolute Shrinkage and Selection Operator	[67]	2021	CT + MRI/CMRI	AUC, accuracy, sensitivity, and specificity rates	161 patients	No

need, models can be developed that generate heatmaps or attention maps to highlight regions of interest in the images. Explainable AI techniques, such as LIME or SHAP, can provide insights into model decisions. *Model Validation and Clinical Trials:* Transitioning from research models to clinical practice requires rigorous validation and testing. Collaboration with medical professionals and institutions to conduct clinical trials and validation studies is essential to demonstrate the model's effectiveness and safety in real-world scenarios. *Real-time Processing:* In a clinical settings, real-time or near-real-time processing of medical images is crucial. To achieve real-time performance, models should be optimized for inference speed, and hardware acceleration options (e.g., GPUs, FPGAs) can be explored.

Addressing these challenges necessitates a multidisciplinary approach involving machine learning experts, medical professionals, data scientists, and regulatory experts to ensure the safe and effective deployment of disease segmentation models in clinical practice.

B. LEARNING MODELS FOR DISEASE SEGMENTATION USING COMPUTER TOMOGRAPHY (CT) IMAGES

In the literature, most studies use Unet models to segment cardiovascular neurocristopathy diseases using CT. Of 15 studies, 8 studies implemented UNet models for segmentation while 2 studies ([82] and [83]) reported the use of GANs for segmentation tasks. The review of the literature indicated that the use of neural networks (especially convolutional neural networks) is also a popular method, frequently implemented for disease-related segmentation tasks.

Regarding performance comparison, no direct comparison of the model's segmentation capability could be achieved because different studies calculated different performance metrics. The most reliable metrics, as calculated in most studies, are sensitivity, specificity, dice score, and Hausdorff distance, along with some other metrics such as accuracy, the Jaccard index, and the calculation of different error values.

Figure 5 demonstrates an example of a segmentation pipeline implemented to segment the true and false lumen in a CT scan image. (0) is the original source image, (1) shows the initial step of the segmentation algorithm that accepts the axial image and performs the localization of the aorta, (2) the centreline identification algorithm is used to derive the aortic centerline, (3) then multiplanar reformations are generated orthogonal to the centerline, (4) and true lumen, false lumen and background is segmented using a segmentation algorithm, (5) the segmented lumen is finally superimposed back on to the axial plane image.

Table 4 summarizes the reviewed literature that performed CT image segmentation using different DL tools. Only two studies, [61] and [85], reported the availability/sharing of the CT image datasets on request.

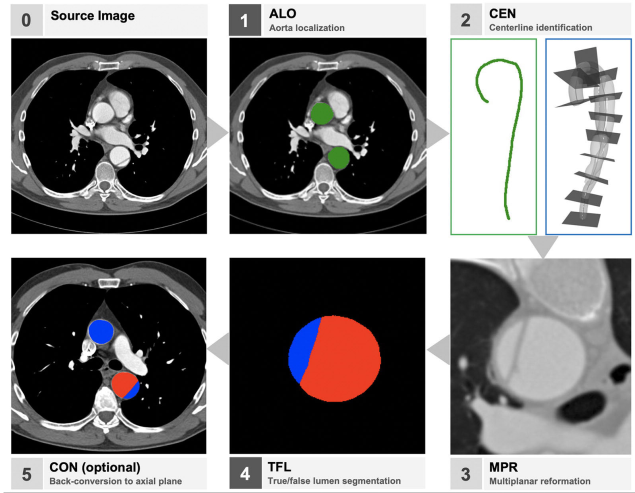

FIGURE 5. Computer Tomography segmentation pipeline. Green = aortic lumen, blue = true lumen, red = false lumen. *Image adapted from [84]: open access.*

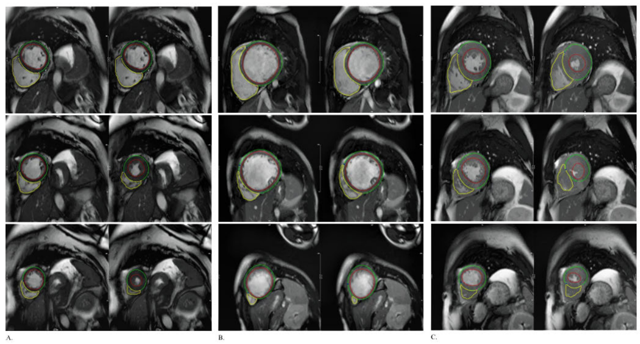

FIGURE 6. Magnetic resonance imaging; Cardiomyopathy segmentation. (A) Images acquired in patients without cardiomyopathy (B) Images acquired in patients with Dilated Cardiomyopathy (DCM) (C) Images acquired in participants with Hypertrophic cardiomyopathy (HCM). *Image Adapted from [93]: open access.*

C. LEARNING MODELS FOR DISEASE SEGMENTATION USING CARDIAC MAGNETIC RESONANCE IMAGING (CMRI)

Most studies in the literature use Unet models to segment cardiovascular neurocristopathy diseases using CMRI/MRI. Figure 6 illustrates an example of automatic left ventricle (LV) segmentation in MRI scans using AI. The sub-figures a,b, and c are the MRI scans of patients without cardiomyopathy, with DCM and with HCM, respectively. The outer edge of the LV is circled in green colour, the red colour circle is an intimal contour of the LV while the yellow colour circle is the intimal contour of the right ventricle.

Table 5 summarizes the reviewed literature on learning models for the segmentation of cardiovascular neurocristopathy disease using DL models, UNet, CNN, and DeepV3+ on the MRI dataset. A dataset of MRI scans of three studies (that is, [59], [60], [94]) could be provided upon reasonable request to the authors.

TABLE 4. Learning models for disease segmentation using Computer Tomography (CT) images.

S.No.	Ref	Data Acquired	Year	Algorithm	Performance	Sample Size		Dataset Availability
						Subjects	Samples	
1	[84]	Stanford University School of Medicine, USA	2020	CNN	Dice similarity coefficient (0.87 +- 0.056)	45	153	No
2	[86]	Chinese PLA General Hospital, the First Affiliated Hospital of Medical College of Zhejiang University, Xiangya Hospital of Central South University, Qilu Hospital of Shandong University, and the Second Peoples Hospital of Yunnan Province, China	2021	CNN	mean Dice score for segmentation of true lumen (0.96), false lumen (0.95) and all branches (0.89)	120	809±119.75	No
3	[87]	Beijing Anzhen Hospital and Fujian Provincial Hospital, China	2021	UNet	Sensitivity score (96%)	154	-	No
4	[69]	University of Palermo, Italy	2021	UNet, ENet, and ERFNet	Sensitivity (91.63%, 92.69%, 89.01%), positive predictive value (91.79, 90.67, 88.41), Dice score (91.09, 91.22, 88.41), volume overlap error (15.30, 15.22, 19.56), relative volume difference (0.12, 2.83, 0.92) and average symmetric surface (5.48, 4.46, 5.48), resp.	72	-	No
5	[85]	The 2nd Affiliated Hospital of Guangzhou Medical University, The First People's Hospital of Foshan and The 2nd Hospital of Shandong University, China	2021	CNN	average Dice coefficient (78.2%)	255	-	On Request
6	[70]	The Rotterdam Study (Database)	2021	Unet	Sensitivity (83.8%), positive predictive value (88.0%) and Correlation coefficient: automatic vs manual (0.98)	1154	2156	No
7	[88]	Peking Union Medical College Hospital (PUMCH), China	2022	Gaussian Naive Bayes	Accuracy, Sensitivity, and Specificity = 0.897, 0.862, and 0.923 (internal test) and 0.730, 0.978 and 0.554 (external testing) cohort	452	-	No
8	[89]	Zhongshan Hospital Fudan University, China	2022	CNN	Dice score (0.903 ± 0.062), Jaccard Index (0.828 ± 0.092) and 95% Hausdorff distance (2.209 ± 2.945)	167	463	No
9	[82]	Quanzhou First Hospital Affiliated to Fujian Medical University, China	2022	GAN + UNet	PSNR (32.98) and SSIM (0.9905)	300	-	No
10	[71]	The Massachusetts General Hospital and Brigham and Women's Hospital Center for Clinical Data Science, USA	2022	UNet	Mean Absolute Error (Model vs Report): Dataset A (Ascending = 0.39 +- 0.59 and Descending = 0.54 +- 0.87); Mean Absolute Error (System vs. Report): Dataset B (Ascending = 0.24 +- 0.38 and Descending = 0.67 +-1.12)	315+1400	-	No
11	[90]	Multiple clinical institution, Japan	2022	Neural Network and UNet	mean Dice coefficient = aortic root (0.95), right-coronary cusp (0.70), left-coronary cusp (0.69), and non-coronary cusp (0.67)	138	258	No
12	[61]	Sun Yat-sen Memorial Hospital of Sun Yat-sen University, China	2022	UNet	Dice Score (0.86), normalized mean absolute error (7.88 +- 4.71) and root mean square error (0.0098 +- 0.0097)	154	-	On Request
13	[91]	Michigan Technological University and Mayo Clinic, USA	2023	UNet	Lumen: Dice score (0.95), relative volume error (0.08), sensitivity (0.97), specificity (1.00), 95% Hausdorff distance (6.64), surface distance (1.11); Intraluminal thrombosis: Dice score (0.80), relative volume error (0.16), sensitivity (0.83), specificity (0.99), 95% Hausdorff distance (6.17), surface distance (1.30)	70	214–2433	No
14	[83]	Oxford University and Oxford University Hospitals National Health Services Foundation Trust, UK	2023	cycle- and conditional GAN	Accuracy (Lumen segmentation) = Cycle-GAN (86.1 +- 12..2); Conditional-GAN (85.7 +- 10.4)	5	11243	No
15	[92]	Hospital's internal radiology database (mPower Clinical Analytics; Nuance Communications, Inc), USA	2023	CNN and VGG-16	Sensitivity (88.3%, 98.9%, 98.7%), specificity (100%, 99.3%, 99.%), accuracy (94.1%, 99.1%, 99.6%) and area under the curve (0.99,0.99,0.99) for selected, balanced and imbalanced image set, respectively.	400	6175	No

TABLE 5. Learning models for disease segmentation using Magnetic Resonance Imaging (MRI).

S.No.	Ref	Data Acquired	Year	Algorithm	Performance	Sample Size		Dataset Availability
						Subjects	Samples	
1	[95]	Lurie Children's Hospital and Northwestern Memorial Hospital, USA	2020	CNN	median Dice score (0.95), Hausdorff distance (2.80) and average symmetrical surface distance (0.176)	1018	-	No
2	[75]	University of Chinese Academy of Science, China (Referral Centre)	2021	DeepV3+	Sensitivity (85.71%), specificity (69.57%), accuracy (78.43%), and AUC (0.80)	198	-	No
3	[93]	Zhongshan Hospital, China	2022	CNN	Sensitivity (92.31% DCM; 78.05%, HCM), specificity (82.96% DCM; 54.07% HCM)	388	-	No
4	[94]	MICCAI 2017 automated cardiac diagnosis challenge (ACDC) dataset	2022	UNet	average Dice coefficients: left ventricle (96.24% diastole, 89.92% systole), right ventricle (92.90% diastole, 86.92% systole)	150	-	Yes
5	[97]	Hospital Virgen de la Arrixaca of Murcia and Hospital Mesa del Castillo of Murcia, Spain	2022	UNet	Dice coefficients for the internal cavity (0.96), external wall (0.89), and trabeculae (0.84); area under the ROC curve (0.94), accuracy (0.87), sensitivity (0.93), and specificity (0.80)	277	-	No
6	[59]	Tertiary care hospital, Korea	2022	UNet	Dice similarity coefficient (0.86 ± 0.05 and 0.74 ± 0.17) for native and post T1 maps, respectively	95	-	On request
7	[60]	UK Biobank dataset	2022	UNet	Correlation	39688	4.6 million	On request
8	[94]	Royal Brompton Hospital in London, UK	2023	UNet	Dice score (0.83 +- 0.05; short-axis, 0.82 +- 0.03; long-axis) and Hausdorff distance (4.0 +- 1.1 mm; short-axis, 7.9 +- 3.9 mm; long-axis)	-	360 short-axis;124 long-axis	On request
9	[98]	University Hospital of Dijon, France	2023	UNet	IoU (96.27%), Dice score (98.09 ± 0.96%) and Hausdorff distance (4.88 ±1.70 mm)	73	30 slices per patients	On request
10	[99]	project 2018-A02010–55 (Comite de Protection des Personnes, France)	2023	UNet	Dice Score (0.90 +- 0.02) and Hausdorff distance (9.58 +- 4.36 mm)	36	-	No

D. LEARNING MODELS FOR DISEASE SEGMENTATION USING X-RAYS AND ECHOCARDIOGRAPHY (ECHO) IMAGES

Limited literature was found on the use of X-rays and echocardiography images for the segmentation of cardiovascular neurocristopathy diseases. One reason could be that frequent exposure to X-rays is harmful to human health. Moreover, echos and X-ray images are of low quality and could only be used for structural segmentation, resulting in relatively less detailed analysis.

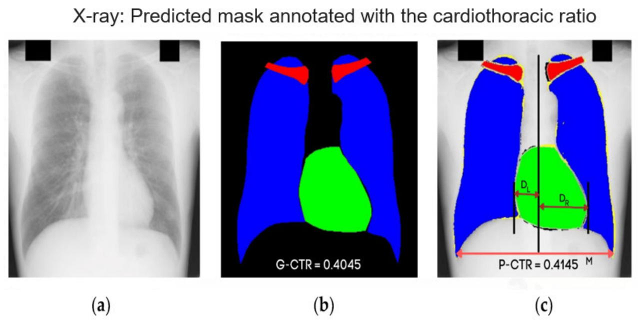

FIGURE 7. **X-ray: Predicted mask annotated with the cardiothoracic ratio. The clavicle (collar bone) is shown in red colour, the lungs in blue and the heart is shown in green colour.** ***Adapted from [100]: open access.***

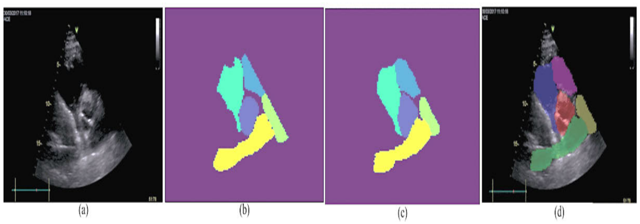

FIGURE 8. **Ultrasound: (a) a TTE image (b) the ground truth (c) the model's prediction and (d) the model's prediction superimposed on the original image. Red: aortic valve (AV), Blue: right atrium/right ventricle (RA/RV), Green: left atrium (LA), Purple: right ventricular outflow tract (RVOT) and Yellow: main pulmonary artery (MPA).** ***Adapted from [101]: open access.***

Figure 7 shows the segmentation of the chest anatomy to calculate the cardiothoracic ratio. (a) shows the original chest X-ray image, (b) is a segmented image using CardioNet, and (c) illustrates the calculation of the maximum width of the heart and thorax using an equation 1.

$$R = (D_L + D_R)/M \tag{1}$$

where R is the cardiothoracic ratio, D_L is heart distance from the left while D_R is heart distance from the right of the central vertical line. M is the maximum horizontal distance between the left and right boundary sides of the lungs, as shown in Figure 7.

Figure 8 shows an example of transesophageal echocardiography (TTE) segmentation. The figure shows the segmentation of the aortic valve, right atrium/right ventricle, left atrium, right ventricular outflow tract and main pulmonary artery. Subfigure (a) is the original TTE image used as an input in the AI model, (b) is the annotated ground truth image, (c) is the model's predicted labels and (d) is the predicted annotations overlayed on the original TTE image.

Table 6 summarizes the literature found on x-rays and echo images for the segmentation of diseases using DL models. The literature reports results using variants of neural networks as DL models. The performance metrics used are accuracy, precision, recall, and F1-score, while some used dice score and IoU. Only one out of 6 studies (that is, [77]) reported the availability of the analyzed dataset on request.

E. IMPLEMENTATION OF DEEP LEARNING MODELS

To build an end-to-end DL model, some open-source informatics resources have been developed, including Keras, TensorFlow, and PyTorch [106]. Keras is a Python/R library that provides high-level functions to build a stack of consecutive layers to form Theano models. Keras library allows the user-friendly network definition, optimization, and effective evaluation of multi-dimensional mathematical expressions. TensorFlow is also a Python/R library developed by the Google team. TensorFlow uses data flow graphs for efficient data processing. Lastly, the PyTorch library, developed by the Meta AI team, works with Python. It is designed to improve the model building and overall data processing speed [43]. Table 7 presents a summarized comparison of the above-mentioned libraries in terms of their architecture, script written, dataset sizes, API levels, do they have trained models, debugging capabilities, and speed performance.

From the reviewed literature, it can be concluded that CNN and Unet (and their variants) are the most frequently used deep learning algorithms. Each algorithm, along with its advantages and limitations, is described as follows:

1) CONVOLUTIONAL NEURAL NETWORKS (CNN)

Convolutional Neural Networks (CNNs) have proven their versatility in various computer vision tasks, including image segmentation. The encoder extracts hierarchical features from the input images through convolutional layers, while the decoder upscales these features to produce pixel-wise segmentation maps. Activation functions like ReLU are common, and loss functions, such as cross-entropy or Dice loss, are employed to optimize the model. Optimization techniques such as stochastic gradient descent (SGD), Adam, RMSprop, or adaptive learning rate algorithms are used for weight updates. Mini-batch training is preferred for improved convergence and memory efficiency. Data augmentation, involving random rotations, flips, and scaling, expands the training dataset and reduces overfitting.

Other elements in CNNs include batch normalization and dropout layers to enhance stability. Architectural modifications like dilated convolutions capture multi-scale features, crucial for certain segmentation tasks. Transfer learning with pre-trained CNN models like VGG or ResNet, fine-tuned for segmentation, has proven effective, especially with limited data.

Advantages of CNNs for segmentation include their adaptability, feature learning capabilities, and fast inference times. However, they may struggle to capture fine details and require substantial labelled data. Overfitting is also a concern, necessitating the use of regularization techniques. Finally, the Interpretability of CNN results can be challenging due to their complex architectures.

2) UNET AND ITS VARIATIONS

U-Net is a specialized architecture specifically designed for image segmentation tasks, with a unique encoder-decoder

TABLE 6. Learning models for disease segmentation using X-rays and Echo-cardiogram (Echo) images.

S.No.	Ref	Data Acquired	Year	Modality	Algorithm	Performance	Sample Size		Dataset Availability
							Subjects	Samples	
1	[77]	Tertiary academic hospitals (Seoul and Gyeonggi-do), Korea	2022	X-rays	ResNet18	Accuracy (90.20%), precision (75.00%), recall (94.44%), and F1-score (83.61%)	3331	3331	On request
2	[102]	Severance Hospital, Yonsei University, Korea	2022	X-rays	EfficientNet and UNet	Precision, Recall, and F1 score were 0.7563, 0.6922, and 0.7176 for all vessels, resp.	38	50	No
3	[103]	INSTITUT JANTUNG NEGARA, Malaysia	2020	Echocardiogram	Unet	Accuracy (99.5%), Precision (86.9%), Recall (96.2%), F1-score (0.91) and IoU (91.1%)	58	247	No
4	[101]	Naval Hospital of Athens, Greece, the First Department of Cardiology of National and Kapodistrian University of Athens, Medical School, Hippokration General Hospital, Greece, and the Cardiology Department of Hippokration General Hospital, Greece	2021	Echocardiogram	CNN and UNet	Accuracy of (97%), sensitivity (94%), specificity (98%), IoU (87%)	97	194	No
5	[104]	Mohammad Hoesin Indonesian General Hospital	2021	Echocardiogram	CNN (Mask-RCNN)	IoU (80%), Dice coefficient similarity (89.7%)	100	1149	No
6	[105]	Wonju Severance Christian Hospital, Wonju, Republic of Korea	2023	Echocardiogram	DNN with attention mechanism and residual features	Dice coefficient (0.90), IoU (082), recall (0.90), precision (0.90)	9	20	No

TABLE 7. Summary comparison of DL libraries: Keras, TensorFlow, and PyTorch.

	Keras	TensorFlow	PyTorch
Architecture	concise, simple, readable	not easy to use	complex, less readable
Written In	Python	Python, C++, CUDA	Lua
Datasets	smaller datasets	large datasets, high performance	large datasets, high performance
API Level	high	high & low	low
Trained Model	yes	yes	yes
Debugging	simple network, no debugging needed	good debugging capability	difficult to conduct debugging
Speed	slow, low performance	fast, high performance	fast, high performance

structure featuring skip connections. The encoder captures high-level features from input images, while the decoder recovers spatial information. The skip connections, a distinctive feature of U-Net, play a crucial role in preserving spatial information during the upsampling process, contributing to accurate segmentation. Common loss functions used for U-Net and its variants include the Dice coefficient or cross-entropy, while optimization often involves techniques like Adam.

U-Net excels in biomedical and general image segmentation tasks, with skip connections enhancing its ability to capture fine details. Variations of U-Net, such as Attention U-Net and ResU-Net, have been developed to further improve performance through attention mechanisms and residual connections. Nevertheless, U-Net and its variations are specialized for segmentation and may not perform optimally in other computer vision tasks. Creating accurate labelled segmentation masks can be labour-intensive and require domain expertise. Overfitting remains a concern, particularly in scenarios with limited data, and complex or noisy images can challenge U-Net's segmentation performance.

IV. FINDINGS

Table 3 summarizes the learning models implemented in the field of cardiovascular neurocristopathy, while Table 4, Table 5 and Table 6 summarize the learning models implemented in the field of cardiovascular neurocristopathy segmentation using CT, MRI, X-rays and echocardiographic images, respectively. The findings of this review article are as follows.

A. STANDARD PERFORMANCE METRICS AND RESULT INTERPRETABILITY

It can be observed from the tables that some studies implemented the same algorithms but reported the segmentation performance using different performance metrics. This makes a fair comparison of these algorithms more complicated, especially if analysed for shortlisting to the most specific and sensitive algorithm that could be implemented in the field of medicine for accurate segmentation purposes. Therefore, it is necessary to standardize performance metrics for ease of comparison and to determine the most accurate segmentation algorithm for each, as well as the most useful imaging modalities.

B. AVAILABILITY OF OPEN-ACCESS DATASETS, ANNOTATION, AND INTERPATIENT VARIABILITY

The review also revealed that there is limited access to publicly available open-access datasets. Only 1 out of 32 studies [57] reported that their data set was open access, while 6 out of 32 studies [59], [60], [61], [77], [85], [94] reported that the data is available to researchers on reasonable request. The limited availability of open-access medical data is subject to privacy and data security. One of the solutions could be the development of standards for data anonymization and following GDPR rules for data sharing across continents.

C. REPRODUCIBILITY OF RESULTS AND HIGH-QUALITY DATASET

For reproducibility of the results, the reporting of data analysis and datasets should also be standardized. Most studies lack reporting of meta-information, for example, the number of sample images within the dataset, preprocessing steps for data cleaning and data analysis. Furthermore, the literature also reports the dependence of segmentation performance on image quality and quantity. For better segmentation performance, the training algorithm needs big data of high-quality detailed images, i.e., a large number of samples per subject and a high number of subjects within the dataset. The availability of patient follow-up images could also help in training the algorithm to learn the pattern of disease progression or regression. Currently, to our knowledge, no such publicly available datasets have multiple images of a large number of patients (ideally millions, as in the UK BioBank [107] which is not free) over the years (follow-ups).

By combined efforts and taking specific actions, computer scientists, engineers, and clinicians can address the limitations mentioned above and develop segmentation tools that are clinically relevant, accurate, and robust.

V. CONCLUSION AND FUTURE DIRECTIONS

Most existing reviews on the topic of cardiovascular neurocristopathy focus on the progression and regression of disease related to abnormal development or migration of cardiac neural crest cells to detect and segment such diseases. The application of machines and DL models in cardiovascular imaging is rapidly increasing with the aim of a possible reduction in reporting time with high precision for the segmentation of cardiovascular neurocristopathy diseases, such as cardiomyopathy, stroke, aorta, and aortic valve dysfunction diseases. In this review, the available literature on the segmentation of cardiovascular neurocristopathy diseases using imaging modalities, such as CT, MRI, X-ray and Echos, is analyzed in terms of implemented segmentation algorithm, performance metrics used, meta-information about the dataset and dataset availability.

From the literature review, it can be concluded and is evident from Table 3, Table 4, Table 5 and Table 6 that Computer Tomography (CT) images are the most commonly used image modality for the segmentation of cardiovascular neurocristopathy disease, while MRI is the second best. Limited literature is available on the use of radiographic (X-ray) and echocardiography (Echo) images for the segmentation of such diseases. This is an open research topic as better imaging equipment has been developed that provides a good quality image that could help in more robust segmentation using these modalities. In terms of the most frequently used DL model, the segmentation using UNet, and its variants, outperform all the other models. UNet is a type of convolutional neural network (CNN) which has features of skip connection (to capture high- and low-level features of image), awareness of spatial context (deals with complex background), symmetric architecture (to capture fine-grained details) and data augmentation ability enabling them to be trained on a smaller dataset. These features make UNet better than other networks in the image segmentation task.

TABLE 8. Specific actions required by engineers and clinicians to address the limitations identified in proposed review.

Problems in segementation	Stackholder	Contribution
Lack of standardised performance metrics, results reporting and interpretability	Clinicians	Help in determining the most relevant metrics to a clinical problem, such as dice score, Hausdorff distance or Jaccard index.
		Help in defining criteria/threshold for acceptable performance, such as minimum specificity and sensitivity
	Engineers	Design/develop and implement shortlisted performance metrics in the segmentation algorithm
		Report the results in standardized formats, such as Medical Image Segmentation Evaluation Framework (MISE) or Segmentation Evaluation Package (SEVAL)
Limited open-access datasets, annotation quality, interpatient variability	Clinicians	Collaborate with engineers to collect and annotate clinical imaging data that represent the problem of cardiovascular neurocristopathies, such as MRI or CT images
		Establish data-sharing agreements with other consortia, hospitals and institutions to increase the size and diversity of the datasets
	Engineers	Develop data augmentation methods to increase data variability and data set size.
		Establish open-access repositories to share the datasets with other research communities
High-quality data and reproducibility of results	Clinicians	Collaborate with engineers to establish guidelines for data annotation and curation to ensure the quality and consistency of the image datasets
		Establish protocols for validation of the results via blind tests or independent reviews to increase the generalizability and reproducibility of the segmentation algorithms
	Engineers	Provide properly documented and open-source code, to facilitate the replication of the results
		Establish reproducible frameworks, such as Reproducible Experiment Platform for Segmentation (REPS), to ensure the reproducibility of the results on different software and hardware platforms

In the literature, Simple CNN is the second most frequently implemented algorithm. While some studies have used adversarial generative networks for the image segmentation task, further investigation into the use of such models is required to get trustworthy/acceptable results.

The review also identified gaps in developing effective disease segmentation models using medical images, especially for critical conditions like cardio-neurocristopathy diseases. Limited data availability, which stems from privacy concerns and the scarcity of expert annotations, necessitates innovative solutions like data augmentation and transfer learning. Ensuring the accuracy and consistency of annotations is critical to mitigate model biases. The diverse interpatient variability in anatomical and pathological aspects underscores the importance of techniques such as data augmentation and domain adaptation to enhance model generalization. Interpretability is crucial for gaining medical professionals' trust, and the incorporation of explainable AI methods can facilitate model transparency. The transition from research to clinical practice involves rigorous validation through collaboration with medical experts and institutions while optimizing models for real-time processing is essential for timely clinical decision-making. Addressing these challenges requires the combined efforts of researchers/engineers and clinicians. Table 8 summarizes the problems and contributions of each stakeholder to overcome these shortcomings.

In the future, in conjunction with collaborative efforts, the use of intravascular ultrasound (IVUS), optical coherence tomography (OCT), and functional magnetic resonance imaging (fMRI) techniques for the detection and segmentation of cardiovascular neurocristopathy disease should also be investigated. IVUS could be used to identify the location and extent of cardiovascular abnormalities associated

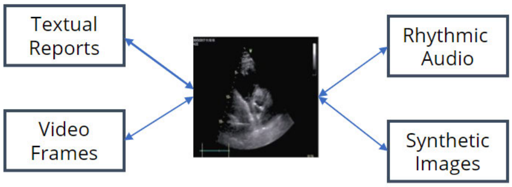

FIGURE 9. Echo-Image based joint embeddings across 4 different modalities using ImageBind model.

with neurocristopathy diseases. Brain activities, such as cognitive deficits, determined by fMRI could be associated with congenital heart disease, a type of cardiovascular neurocristopathy. OCT imaging could help visualize the microstructure of blood vessels within the heart and identify abnormalities in the cardiovascular system associated with neurocristopathy diseases. All of these techniques may not provide direct visualization of abnormalities in the cardiovascular system, but a correlation can be derived from their analysis that could help clinicians in the early detection of cardiovascular neurocristopathy diseases.

Furthermore, Meta AI has proposed an ImageBind model [108] that capitalizes on image-paired data to create a unified representation space. An example of such a model is shown in Figure 9. The ImageBind model learns joint embeddings across six different modalities which are image, audio, depth, text, thermal and Inertial Measurement Unit (IMU) data. Utilizing such a model, a medical data-based model could be designed in the future that could generate the cardiac parameters (cardiac rhythm, beat sound) and medical reports from a single image (CT, MRI, X-ray and/or Echo) using a few-shot DL approach, reducing the cost of healthcare and providing an efficient diagnosis.

REFERENCES

[1] G. A. Roth et al., "Global burden of cardiovascular diseases and risk factors, 1990–2019: Update from the GBD 2019 study," *J. Amer. College Cardiol.*, vol. 76, no. 25, pp. 2982–3021, 2020.

[2] G. A. Vega-Lopez, S. Cerrizuela, C. Tribulo, and M. J. Aybar, "Neurocristopathies: New insights 150 years after the neural crest discovery," *Develop. Biol.*, vol. 444, pp. 110–143, Dec. 2018.

[3] M. E. Barnes. (Nov. 2014). *The Embryo Project Encyclopedia*. [Online]. Available: https://embryo.asu.edu/handle/10776/8202

[4] T. S. Sato, A. Handa, S. Priya, P. Watal, R. M. Becker, and Y. Sato, "Neurocristopathies: Enigmatic appearances of neural crest cell-derived abnormalities," *RadioGraphics*, vol. 39, no. 7, pp. 2085–2102, Nov. 2019.

[5] P. Lacaze, R. Sebra, M. Riaz, J. Ingles, J. Tiller, B. A. Thompson, P. A. James, D. Fatkin, C. Semsarian, C. M. Reid, A. M. Tonkin, I. Winship, E. Schadt, and J. J. McNeil, "Genetic variants associated with inherited cardiovascular disorders among 13,131 asymptomatic older adults of European descent," *npj Genomic Med.*, vol. 6, no. 1, p. 51, Jun. 2021.

[6] C. De Bono, Y. Liu, A. Ferrena, A. Valentine, D. Zheng, and B. E. Morrow, "Single-cell transcriptomics uncovers a non-autonomous *Tbx1*-dependent genetic program controlling cardiac neural crest cell development," *Nature Commun.*, vol. 14, no. 1, p. 1551, Mar. 2023.

[7] B. Grygiel-Górniak, M.-T. Oduah, A. Olagunju, and M. Klokner, "Disorders of the aorta and aortic valve in connective tissue diseases," *Current Cardiol. Rep.*, vol. 22, no. 8, pp. 1–14, Aug. 2020.

[8] C. Chen, C. Qin, H. Qiu, G. Tarroni, J. Duan, W. Bai, and D. Rueckert, "Deep learning for cardiac image segmentation: A review," *Frontiers Cardiovascular Med.*, vol. 7, p. 25, Mar. 2020.

[9] N. Pilon, "Treatment and prevention of neurocristopathies," *Trends Mol. Med.*, vol. 27, no. 5, pp. 451–468, May 2021.

[10] M. Sattur, A. R. Pines, and B. R. Bendok, "Thinking from the heart: Neurocristopathy, aortic abnormalities, and intracranial aneurysms," *World Neurosurg.*, vol. 85, pp. 25–27, Jan. 2016.

[11] E. M. Isselbacher et al., "2022 ACC/AHA guideline for the diagnosis and management of aortic disease: A report of the American Heart Association/American College of Cardiology joint committee on clinical practice guidelines," *J. Amer. College Cardiol.*, vol. 80, no. 24, pp. 223–393, Dec. 2022.

[12] A. S. Helms, A. D. Thompson, and S. M. Day, "Translation of new and emerging therapies for genetic cardiomyopathies," *JACC, Basic Transl. Sci.*, vol. 7, no. 1, pp. 70–83, Jan. 2022.

[13] (Mar. 2022). *Cardiomyopathy Types*. [Online]. Available: https://www.nhlbi.nih.gov/health/cardiomyopathy/types

[14] Y.-H. Lian, X. Chen, D.-R. Kong, W. Chen, M.-C. Shi, and H.-W. Zhou, "Cervical artery dissection—An easily neglected cause of stroke: A case report," *BMC Neurol.*, vol. 20, no. 1, p. 428, Nov. 2020.

[15] S.-C. Huang, A. Pareek, S. Seyyedi, I. Banerjee, and M. P. Lungren, "Fusion of medical imaging and electronic health records using deep learning: A systematic review and implementation guidelines," *npj Digit. Med.*, vol. 3, no. 1, p. 136, Oct. 2020.

[16] Y. Kumar, A. Koul, R. Singla, and M. F. Ijaz, "Artificial intelligence in disease diagnosis: A systematic literature review, synthesizing framework and future research agenda," *J. Ambient Intell. Humanized Comput.*, vol. 15, pp. 8459–8486, Jan. 2022.

[17] M. M. Ahsan and Z. Siddique, "Machine learning-based heart disease diagnosis: A systematic literature review," *Artif. Intell. Med.*, vol. 128, Jun. 2022, Art. no. 102289.

[18] M. T. Tsakok and F. V. Gleeson, "The chest radiograph in heart disease," *Medicine*, vol. 46, no. 8, pp. 453–457, Aug. 2018.

[19] (Jun. 2022). *X-Rays*. [Online]. Available: https://www.nibib.nih.gov/science-education/science-topics/x-rays

[20] R. Hajhosseiny, I. Rashid, A. Bustin, C. Munoz, G. Cruz, M. S. Nazir, K. Grigoryan, T. F. Ismail, R. Preston, R. Neji, K. Kunze, R. Razavi, A. Chiribiri, P. G. Masci, R. Rajani, C. Prieto, and R. M. Botnar, "Clinical comparison of sub-mm high-resolution non-contrast coronary CMR angiography against coronary CT angiography in patients with low-intermediate risk of coronary artery disease: A single center trial," *J. Cardiovascular Magn. Reson.*, vol. 23, no. 1, p. 57, Dec. 2021.

[21] H. Lee, S. Martin, J. R. Burt, P. S. Bagherzadeh, S. Rapaka, H. N. Gray, T. J. Leonard, C. Schwemmer, and U. J. Schoepf, "Machine learning and coronary artery calcium scoring," *Current Cardiol. Rep.*, vol. 22, no. 9, pp. 1–6, Sep. 2020.

[22] V. Russo, L. Lovato, and G. Ligabue, "Cardiac MRI: Technical basis," *La Radiologia Medica*, vol. 125, no. 11, pp. 1040–1055, Nov. 2020.

[23] A. E. Campbell-Washburn et al., "Opportunities in interventional and diagnostic imaging by using high-performance low-field-strength MRI," *Radiology*, vol. 293, no. 2, pp. 384–393, Nov. 2019.

[24] A. Vieillard-Baron, S. J. Millington, F. Sanfilippo, M. Chew, J. Diaz-Gomez, A. McLean, M. R. Pinsky, J. Pulido, P. Mayo, and N. Fletcher, "A decade of progress in critical care echocardiography: A narrative review," *Intensive Care Med.*, vol. 45, no. 6, pp. 770–788, Jun. 2019.

[25] S. P. Power, F. Moloney, M. Twomey, K. James, O. J. O'Connor, and M. M. Maher, "Computed tomography and patient risk: Facts, perceptions and uncertainties," *World J. Radiol.*, vol. 8, no. 12, p. 902, 2016.

[26] E. Maffei, S. Seitun, C. Martini, A. Aldrovandi, G. Cervellin, C. Tedeschi, A. Guaricci, G. Messalli, O. Catalano, and F. Cademartiri, "Prognostic value of computed tomography coronary angiography in patients with chest pain of suspected cardiac origin," *La Radiologia Medica*, vol. 116, no. 5, pp. 690–705, Aug. 2011.

[27] A. I. Guaricci, G. Pontone, L. Fusini, M. De Luca, F. P. Cafarelli, M. Guglielmo, A. Baggiano, V. Beltrama, G. Muscogiuri, S. Mushtaq, E. Conte, G. Guglielmi, D. Andreini, N. D. Brunetti, M. Di Biase, A. L. Bartorelli, and M. Pepi, "Additional value of inflammatory biomarkers and carotid artery disease in prediction of significant coronary artery disease as assessed by coronary computed tomography angiography," *Eur. Heart J. Cardiovascular Imag.*, vol. 18, no. 9, pp. 1049–1056, Sep. 2017.

[28] A. I. Guaricci, T. Arcadi, N. D. Brunetti, E. Maffei, D. Montrone, C. Martini, M. De Luca, F. De Rosa, D. Cocco, M. Midiri, F. Cademartiri, L. Macarini, M. Di Biase, and G. Pontone, "Carotid intima media thickness and coronary atherosclerosis linkage in symptomatic intermediate risk patients evaluated by coronary computed tomography angiography," *Int. J. Cardiol.*, vol. 176, no. 3, pp. 988–993, Oct. 2014.

[29] G. Pontone et al., "Prognostic stratification of patients with ST-segment–elevation myocardial infarction (PROSPECT): A cardiac magnetic resonance study," *Circulat., Cardiovascular Imag.*, vol. 10, no. 11, Nov. 2017, Art. no. e006428.

[30] N. Gaibazzi, T. Porter, V. Lorenzoni, G. Pontone, D. De Santis, A. De Rosa, and A. I. Guaricci, "Effect of coronary revascularization on the prognostic value of stress myocardial contrast wall motion and perfusion imaging," *J. Amer. Heart Assoc.*, vol. 6, no. 6, Nov. 2017, Art. no. e006202.

[31] M. Guglielmo, A. Baggiano, G. Muscogiuri, L. Fusini, D. Andreini, S. Mushtaq, E. Conte, A. Annoni, A. Formenti, E. M. Mancini, P. Gripari, A. I. Guaricci, M. G. Rabbat, M. Pepi, and G. Pontone, "Multimodality imaging of left atrium in patients with atrial fibrillation," *J. Cardiovascular Comput. Tomogr.*, vol. 13, no. 6, pp. 340–346, Nov. 2019.

[32] M. Guglielmo et al., "T1 mapping and cardiac magnetic resonance feature tracking in mitral valve prolapse," *Eur. Radiol.*, vol. 31, no. 2, pp. 1100–1109, Feb. 2021.

[33] G. Pontone, A. I. Guaricci, S. C. Palmer, D. Andreini, M. Verdecchia, L. Fusini, V. Lorenzoni, M. Guglielmo, G. Muscogiuri, A. Baggiano, M. G. Rabbat, F. Cademartiri, and G. F. Strippoli, "Diagnostic performance of non-invasive imaging for stable coronary artery disease: A meta-analysis," *Int. J. Cardiol.*, vol. 300, pp. 276–281, Feb. 2020.

[34] S. Motoyama, H. Ito, M. Sarai, T. Kondo, H. Kawai, Y. Nagahara, H. Harigaya, S. Kan, H. Anno, H. Takahashi, H. Naruse, J. Ishii, H. Hecht, L. J. Shaw, Y. Ozaki, and J. Narula, "Plaque characterization by coronary computed tomography angiography and the likelihood of acute coronary events in mid-term follow-up," *J. Amer. College Cardiol.*, vol. 66, no. 4, pp. 337–346, Jul. 2015.

[35] E. Maffei, S. Seitun, C. Martini, A. Palumbo, G. Tarantini, E. Berti, R. Grilli, C. Tedeschi, G. Messalli, A. Guaricci, A. C. Weustink, N. R. Mollet, and F. Cademartiri, "CT coronary angiography and exercise ECG in a population with chest pain and low-to-intermediate pre-test likelihood of coronary artery disease," *Heart*, vol. 96, no. 24, pp. 1973–1979, Dec. 2010.

[36] M. van Assen, G. Muscogiuri, D. Caruso, S. J. Lee, A. Laghi, and C. N. De Cecco, "Artificial intelligence in cardiac radiology," *La Radiologia Medica*, vol. 125, pp. 1186–1199, Sep. 2020.

[37] S. Moccia, R. Banali, C. Martini, G. Muscogiuri, G. Pontone, M. Pepi, and E. G. Caiani, "Development and testing of a deep learning-based strategy for scar segmentation on CMR-LGE images," *Magn. Reson. Mater. Phys., Biol. Med.*, vol. 32, no. 2, pp. 187–195, Apr. 2019.

[38] G. Muscogiuri, M. Van Assen, C. Tesche, C. N. De Cecco, M. Chiesa, S. Scafuri, M. Guglielmo, A. Baggiano, L. Fusini, A. I. Guaricci, M. G. Rabbat, and G. Pontone, "Artificial intelligence in coronary computed tomography angiography: From anatomy to prognosis," *BioMed Res. Int.*, vol. 2020, Dec. 2020, Art. no. 6649410.

[39] J. R. England and P. M. Cheng, "Artificial intelligence for medical image analysis: A guide for authors and reviewers," *Amer. J. Roentgenol.*, vol. 212, no. 3, pp. 513–519, Mar. 2019.

[40] P. Sharma, M. Suehling, T. Flohr, and D. Comaniciu, "Artificial intelligence in diagnostic imaging: Status quo, challenges, and future opportunities," *J. Thoracic Imag.*, vol. 35, pp. 11–16, May 2020.

[41] B. Jiang, N. Guo, Y. Ge, L. Zhang, M. Oudkerk, and X. Xie, "Development and application of artificial intelligence in cardiac imaging," *Brit. J. Radiol.*, vol. 93, no. 1113, Sep. 2020, Art. no. 20190812.

[42] T. Infante, C. Cavaliere, B. Punzo, V. Grimaldi, M. Salvatore, and C. Napoli, "Radiogenomics and artificial intelligence approaches applied to cardiac computed tomography angiography and cardiac magnetic resonance for precision medicine in coronary heart disease: A systematic review," *Circulat., Cardiovascular Imag.*, vol. 14, no. 12, pp. 1133–1146, Dec. 2021.

[43] G. Muscogiuri, V. Volpato, R. Cau, M. Chiesa, L. Saba, M. Guglielmo, A. Senatieri, G. Chierchia, G. Pontone, S. Dell'Aversana, U. J. Schoepf, M. G. Andrews, P. Basile, A. I. Guaricci, P. Marra, D. Muraru, L. P. Badano, and S. Sironib, "Application of AI in cardiovascular multimodality imaging," *Heliyon*, vol. 8, no. 10, Oct. 2022, Art. no. e10872.

[44] D. Mastrodicasa, M. Codari, K. Bäumler, V. Sandfort, J. Shen, G. Mistelbauer, L. D. Hahn, V. L. Turner, B. Desjardins, M. J. Willemink, and D. Fleischmann, "Artificial intelligence applications in aortic dissection imaging," *Seminars Roentgenol.*, vol. 57, no. 4, pp. 357–363, Oct. 2022.

[45] *Welcome to the Preferred Reporting Items for Systematic Reviews and Meta-Analyses (PRISMA) Website!*, PRISMA, Berlin, Germany, 2021.

[46] I. Landi, B. S. Glicksberg, H.-C. Lee, S. Cherng, G. Landi, M. Danieletto, J. T. Dudley, C. Furlanello, and R. Miotto, "Deep representation learning of electronic health records to unlock patient stratification at scale," *npj Digit. Med.*, vol. 3, no. 1, p. 96, Jul. 2020.

[47] D. Zhang, C. Yin, J. Zeng, X. Yuan, and P. Zhang, "Combining structured and unstructured data for predictive models: A deep learning approach," *BMC Med. Informat. Decis. Making*, vol. 20, no. 1, pp. 1–11, Dec. 2020.

[48] D. R. Sarvamangala and R. V. Kulkarni, "Convolutional neural networks in medical image understanding: A survey," *Evol. Intell.*, vol. 15, no. 1, pp. 1–22, Mar. 2022.

[49] J. Teuho, J. Schultz, R. Klén, J. Knuuti, A. Saraste, N. Ono, and S. Kanaya, "Classification of ischemia from myocardial polar maps in ^{15}O–H_2O cardiac perfusion imaging using a convolutional neural network," *Sci. Rep.*, vol. 12, no. 1, p. 2839, Feb. 2022.

[50] T. Iqbal and H. Ali, "Generative adversarial network for medical images (MI-GAN)," *J. Med. Syst.*, vol. 42, no. 11, pp. 1–11, Nov. 2018.

[51] J. Bertels, D. Robben, R. Lemmens, and D. Vandermeulen, "Convolutional neural networks for medical image segmentation," 2022, *arXiv:2211.09562*.

[52] K. S. Shakya, A. Laddi, and M. Jaiswal, "Automated methods for sella turcica segmentation on cephalometric radiographic data using deep learning (CNN) techniques," *Oral Radiol.*, vol. 39, no. 2, pp. 248–265, Apr. 2023.

[53] R. W. Pettit, B. B. Marlatt, S. J. Corr, J. Havelka, and A. Rana, "nnU-Net deep learning method for segmenting parenchyma and determining liver volume from computed tomography images," *Ann. Surgery Open*, vol. 3, no. 2, p. e155, Jun. 2022.

[54] D. Müller, I. Soto-Rey, and F. Kramer, "Towards a guideline for evaluation metrics in medical image segmentation," *BMC Res. Notes*, vol. 15, no. 1, pp. 1–8, Dec. 2022.

[55] S. Chaganti, P. Grenier, A. Balachandran, G. Chabin, S. Cohen, T. Flohr, B. Georgescu, S. Grbic, S. Liu, F. Mellot, N. Murray, S. Nicolaou, W. Parker, T. Re, P. Sanelli, A. W. Sauter, Z. Xu, Y. Yoo, V. Ziebandt, and D. Comaniciu, "Automated quantification of CT patterns associated with COVID-19 from chest CT," *Radiol., Artif. Intell.*, vol. 2, no. 4, Jul. 2020, Art. no. e200048.

[56] H. Wang, T. Qu, K. Bernstein, D. Barbee, and D. Kondziolka, "Automatic segmentation of vestibular schwannomas from T1-weighted MRI with a deep neural network," *Radiat. Oncol.*, vol. 18, no. 1, pp. 1–9, May 2023.

[57] T. Guo, Z. Fang, G. Yang, Y. Zhou, N. Ding, W. Peng, X. Gong, H. He, X. Pan, and X. Chai, "Machine learning models for predicting in-hospital mortality in acute aortic dissection patients," *Frontiers Cardiovascular Med.*, vol. 8, Sep. 2021, Art. no. 727773.

[58] S. Jiang, L. Zhang, J. Wang, X. Li, S. Hu, Y. Fu, X. Wang, S. Hao, and C. Hu, "Differentiating between cardiac amyloidosis and hypertrophic cardiomyopathy on non-contrast cine-magnetic resonance images using machine learning-based radiomics," *Frontiers Cardiovascular Med.*, vol. 9, Oct. 2022, Art. no. 1001269.

[59] S. Chang, K. Han, S. Lee, Y. J. Yang, P. K. Kim, B. W. Choi, and Y. J. Suh, "Automated measurement of native T1 and extracellular volume fraction in cardiac magnetic resonance imaging using a commercially available deep learning algorithm," *Korean J. Radiol.*, vol. 23, no. 12, pp. 1251–1259, Dec. 2022.

[60] J. P. Pirruccello et al., "Deep learning enables genetic analysis of the human thoracic aorta," *Nature Genet.*, vol. 54, no. 1, pp. 40–51, Jan. 2022.

[61] L. Lv, H. Li, Z. Wu, W. Zeng, P. Hua, and S. Yang, "An artificial intelligence-based platform for automatically estimating time-averaged wall shear stress in the ascending aorta," *Eur. Heart J. Digit. Health*, vol. 3, no. 4, pp. 525–534, Dec. 2022.

[62] S. X. Morita, K. Kusunose, A. Haga, M. Sata, K. Hasegawa, Y. Raita, M. P. Reilly, M. A. Fifer, M. S. Maurer, and Y. J. Shimada, "Deep learning analysis of echocardiographic images to predict positive genotype in patients with hypertrophic cardiomyopathy," *Frontiers Cardiovascular Med.*, vol. 8, Aug. 2021, Art. no. 669860.

[63] A. Asif, P. F. P. Charters, C. A. S. Thompson, H. M. E. I. Komber, B. J. Hudson, and J. C. L. Rodrigues, "Artificial intelligence can detect left ventricular dilatation on contrast-enhanced thoracic computer tomography relative to cardiac magnetic resonance imaging," *Brit. J. Radiol.*, vol. 95, no. 1138, Oct. 2022, Art. no. 20210852.

[64] Y. Lee, B. Choi, M. S. Lee, U. Jin, S. Yoon, Y.-Y. Jo, and J.-M. Kwon, "An artificial intelligence electrocardiogram analysis for detecting cardiomyopathy in the peripartum period," *Int. J. Cardiol.*, vol. 352, pp. 72–77, Apr. 2022.

[65] D. K. Lee, J. H. Kim, J. Oh, T. H. Kim, M. S. Yoon, D. J. Im, J. H. Chung, and H. Byun, "Deep learning algorithms for detecting acute thoracic aortic dissection on plain chest radiography: A retrospective multicenter study," *Sci. Rep.*, vol. 12, p. 21884, Dec. 2022.

[66] H. Zhao, Z. Xu, Y. Zhu, R. Xue, J. Wang, J. Ren, W. Wang, W. Duan, and M. Zheng, "The construction of a risk prediction model based on neural network for pre-operative acute ischemic stroke in acute type a aortic dissection patients," *Frontiers Neurol.*, vol. 12, Dec. 2021, Art. no. 792678.

[67] L. Qin, C. Chen, S. Gu, M. Zhou, Z. Xu, Y. Ge, F. Yan, and W. Yang, "A radiomic approach to predict myocardial fibrosis on coronary CT angiography in hypertrophic cardiomyopathy," *Int. J. Cardiol.*, vol. 337, pp. 113–118, Aug. 2021.

[68] J. L. Walsh, W. A. AlJaroudi, N. Lamaa, O. K. A. Hassan, K. Jalkh, I. H. Elhajj, G. Sakr, and H. Isma'eel, "A speckle-tracking strain-based artificial neural network model to differentiate cardiomyopathy type," *Scandin. Cardiovascular J.*, vol. 54, no. 2, pp. 92–99, Mar. 2020.

[69] A. Comelli, N. Dahiya, A. Stefano, V. Benfante, G. Gentile, V. Agnese, G. M. Raffa, M. Pilato, A. Yezzi, G. Petrucci, and S. Pasta, "Deep learning approach for the segmentation of aneurysmal ascending aorta," *Biomed. Eng. Lett.*, vol. 11, no. 1, pp. 15–24, Feb. 2021.

[70] G. Bortsova, D. Bos, F. Dubost, M. W. Vernooij, M. K. Ikram, G. van Tulder, and M. de Bruijne, "Automated segmentation and volume measurement of intracranial internal carotid artery calcification at noncontrast CT," *Radiol., Artif. Intell.*, vol. 3, no. 5, Sep. 2021, Art. no. e200226.

[71] F. B. D. C. Macruz, C. Lu, J. Strout, A. Takigami, R. Brooks, S. Doyle, M. Yun, V. Buch, S. Hedgire, and B. Ghoshhajra, "Quantification of the thoracic aorta and detection of aneurysm at CT: Development and validation of a fully automatic methodology," *Radiol., Artif. Intell.*, vol. 4, no. 2, Mar. 2022, Art. no. e210076.

[72] S. Goto, D. Solanki, J. E. John, R. Yagi, M. Homilius, G. Ichihara, Y. Katsumata, H. K. Gaggin, Y. Itabashi, C. A. MacRae, and R. C. Deo, "Multinational federated learning approach to train ECG and echocardiogram models for hypertrophic cardiomyopathy detection," *Circulation*, vol. 146, no. 10, pp. 755–769, Sep. 2022.

[73] R. Cau, F. Pisu, M. Porcu, F. Cademartiri, R. Montisci, P. Bassareo, G. Muscogiuri, A. Amadu, S. Sironi, A. Esposito, J. S. Suri, and L. Saba, "Machine learning approach in diagnosing Takotsubo cardiomyopathy: The role of the combined evaluation of atrial and ventricular strain, and parametric mapping," *Int. J. Cardiol.*, vol. 373, pp. 124–133, Feb. 2023.

[74] M. D. T. de Melo, J. D. A. B. Araujo-Filho, J. R. Barbosa, C. Rocon, C. D. M. Regis, A. dos Santos Felix, R. K. Filho, E. A. Bocchi, L. A. Hajjar, M. Tabassian, J. D'hooge, and V. M. C. Salemi, "A machine learning framework for the evaluation of myocardial rotation in patients with noncompaction cardiomyopathy," *PLoS One*, vol. 16, no. 11, Nov. 2021, Art. no. e0260195.

[75] H. Zhou, L. Li, Z. Liu, K. Zhao, X. Chen, M. Lu, G. Yin, L. Song, S. Zhao, H. Zheng, and J. Tian, "Deep learning algorithm to improve hypertrophic cardiomyopathy mutation prediction using cardiac cine images," *Eur. Radiol.*, vol. 31, no. 6, pp. 3931–3940, Jun. 2021.

[76] H. Wu, Z. Huang, J. Liu, J. Dai, Y. Zhao, and W. Luo, "The predictive value of deep learning-based cardiac ultrasound flow imaging for hypertrophic cardiomyopathy complicating arrhythmias," *Eur. J. Med. Res.*, vol. 28, no. 1, pp. 1–10, Jan. 2023.

[77] D. K. Lee, J. H. Kim, J. Oh, T. H. Kim, M. S. Yoon, D. J. Im, J. H. Chung, and H. Byun, "Detection of acute thoracic aortic dissection based on plain chest radiography and a residual neural network (Resnet)," *Sci. Rep.*, vol. 12, no. 1, p. 21884, Dec. 2022.

[78] D. Alis, A. Guler, M. Yergin, and O. Asmakutlu, "Assessment of ventricular tachyarrhythmia in patients with hypertrophic cardiomyopathy with machine learning-based texture analysis of late gadolinium enhancement cardiac MRI," *Diagnostic Interventional Imag.*, vol. 101, no. 3, pp. 137–146, Mar. 2020.

[79] O. Irtyuga, G. Kopanitsa, A. Kostareva, O. Metsker, V. Uspensky, G. Mikhail, G. Faggian, G. Sefieva, I. Derevitskii, A. Malashicheva, and E. Shlyakhto, "Application of machine learning methods to analyze occurrence and clinical features of ascending aortic dilatation in patients with and without bicuspid aortic valve," *J. Personalized Med.*, vol. 12, no. 5, p. 794, May 2022.

[80] C. Rocon, M. Tabassian, M. D. T. de Melo, J. A. de Araujo Filho, C. J. Grupi, J. R. Parga Filho, E. A. Bocchi, J. D'hooge, and V. M. C. Salemi, "Biventricular imaging markers to predict outcomes in non-compaction cardiomyopathy: A machine learning study," *ESC Heart Failure*, vol. 7, no. 5, pp. 2431–2439, Oct. 2020.

[81] W.-L. Peng, T.-J. Zhang, K. Shi, H.-X. Li, Y. Li, S. He, C. Li, D. Xia, C.-C. Xia, and Z.-L. Li, "Automatic machine learning based on native T1 mapping can identify myocardial fibrosis in patients with hypertrophic cardiomyopathy," *Eur. Radiol.*, vol. 32, pp. 1044–1053, Sep. 2022.

[82] H. Chen, S. Yan, M. Xie, and J. Huang, "Application of cascaded GAN based on CT scan in the diagnosis of aortic dissection," *Comput. Methods Programs Biomed.*, vol. 226, Nov. 2022, Art. no. 107130.

[83] A. Chandrashekar, A. Handa, P. Lapolla, N. Shivakumar, R. Uberoi, V. Grau, and R. Lee, "A deep learning approach to visualize aortic aneurysm morphology without the use of intravenous contrast agents," *Ann. Surg.*, vol. 277, no. 2, pp. 449–459, Feb. 2023.

[84] L. D. Hahn, G. Mistelbauer, K. Higashigaito, M. Koci, M. J. Willemink, A. M. Sailer, M. Fischbein, and D. Fleischmann, "CT-based true- and false-lumen segmentation in type B aortic dissection using machine learning," *Radiol., Cardiothoracic Imag.*, vol. 2, no. 3, Jun. 2020, Art. no. e190179.

[85] J. Hou, M. Y. Gao, A. Z. Pan, Q. D. Wang, B. Liu, Y. B. Jin, J. B. Lu, Q. Y. He, X. D. Zhang, and W. Wang, "Relationship between circle of Willis variations and cerebral or cervical arteries stenosis investigated by computer tomography angiography and multitask convolutional neural network," *J. Healthcare Eng.*, vol. 2021, Oct. 2021, Art. no. 6024352.

[86] D. Chen, X. Zhang, Y. Mei, F. Liao, H. Xu, Z. Li, Q. Xiao, W. Guo, H. Zhang, T. Yan, J. Xiong, and Y. Ventikos, "Multi-stage learning for segmentation of aortic dissections using a prior aortic anatomy simplification," *Med. Image Anal.*, vol. 69, Apr. 2021, Art. no. 101931.

[87] X. Xiong, X. Guan, C. Sun, T. Zhang, H. Chen, Y. Ding, Z. Cheng, L. Zhao, X. Ma, and G. Xie, "A cascaded deep learning framework for detecting aortic dissection using non-contrast enhanced computed tomography," in *Proc. 43rd Annu. Int. Conf. IEEE Eng. Med. Biol. Soc. (EMBC)*, Nov. 2021, pp. 2914–2917.

[88] Y. Yi, L. Mao, C. Wang, Y. Guo, X. Luo, D. Jia, Y. Lei, J. Pan, J. Li, S. Li, X.-L. Li, Z. Jin, and Y. Wang, "Advanced warning of aortic dissection on non-contrast CT: The combination of deep learning and morphological characteristics," *Frontiers Cardiovascular Med.*, vol. 8, p. 1910, Jan. 2022.

[89] H. Feng, Z. Fu, Y. Wang, P. Zhang, H. Lai, and J. Zhao, "Automatic segmentation of thrombosed aortic dissection in post-operative CT-angiography images," *Med. Phys.*, vol. 50, no. 6, pp. 3538–3548, Jun. 2023.

[90] G. Aoyama, L. Zhao, S. Zhao, X. Xue, Y. Zhong, H. Yamauchi, H. Tsukihara, E. Maeda, K. Ino, N. Tomii, S. Takagi, I. Sakuma, M. Ono, and T. Sakaguchi, "Automatic aortic valve cusps segmentation from CT images based on the cascading multiple deep neural networks," *J. Imag.*, vol. 8, no. 1, p. 11, Jan. 2022.

[91] N. Mu, Z. Lyu, M. Rezaeitaleshmahalleh, X. Zhang, T. Rasmussen, R. McBane, and J. Jiang, "Automatic segmentation of abdominal aortic aneurysms from CT angiography using a context-aware cascaded U-Net," *Comput. Biol. Med.*, vol. 158, May 2023, Art. no. 106569.

[92] R. T. Tomihama, J. R. Camara, and S. C. Kiang, "Machine learning analysis of confounding variables of a convolutional neural network specific for abdominal aortic aneurysms," *JVS-Vascular Sci.*, vol. 4, Jan. 2023, Art. no. 100096.

[93] J. Guo, H. Lu, Y. Chen, M. Zeng, and H. Jin, "Artificial intelligence study on left ventricular function among normal individuals, hypertrophic cardiomyopathy and dilated cardiomyopathy patients using 1.5T cardiac cine MR images obtained by SSFP sequence," *Brit. J. Radiol.*, vol. 95, no. 1133, May 2022, Art. no. 20201060.

[94] H. Barbaroux, K. P. Kunze, R. Neji, M. S. Nazir, D. J. Pennell, S. Nielles-Vallespin, A. D. Scott, and A. A. Young, "Automated segmentation of long and short axis DENSE cardiovascular magnetic resonance for myocardial strain analysis using spatio-temporal convolutional neural networks," *J. Cardiovascular Magn. Reson.*, vol. 25, no. 1, pp. 1–17, Mar. 2023.

[95] H. Berhane, M. Scott, M. Elbaz, K. Jarvis, P. McCarthy, J. Carr, C. Malaisrie, R. Avery, A. J. Barker, J. D. Robinson, C. K. Rigsby, and M. Markl, "Fully automated 3D aortic segmentation of 4D flow MRI for hemodynamic analysis using deep learning," *Magn. Reson. Med.*, vol. 84, no. 4, pp. 2204–2218, Oct. 2020.

[96] A. Wibowo, P. Triadyaksa, A. Sugiharto, E. A. Sarwoko, F. A. Nugroho, H. Arai, and M. Kawakubo, "Cardiac disease classification using two-dimensional thickness and few-shot learning based on magnetic resonance imaging image segmentation," *J. Imag.*, vol. 8, no. 7, p. 194, Jul. 2022.

[97] J. M. Rodríguez-de-Vera, G. Bernabé, J. M. García, D. Saura, and J. González-Carrillo, "Left ventricular non-compaction cardiomyopathy automatic diagnosis using a deep learning approach," *Comput. Methods Programs Biomed.*, vol. 214, Feb. 2022, Art. no. 106548.

[98] E. Markodimitrakis, S. Lin, E. Koutoulakis, D. M. Marín-Castrillón, F. A. T. Sáez, S. Leclerc, C. Bernard, A. Boucher, B. Presles, O. Bouchot, T. Decourselle, M.-C. Morgant, and A. Lalande, "Comparison of in-vivo and ex-vivo ascending aorta elastic properties through automatic deep learning segmentation of cine-MRI and biomechanical testing," *J. Clin. Med.*, vol. 12, no. 2, p. 402, Jan. 2023.

[99] D. M. Marin-Castrillon, A. Lalande, S. Leclerc, K. Ambarki, M.-C. Morgant, A. Cochet, S. Lin, O. Bouchot, A. Boucher, and B. Presles, "4D segmentation of the thoracic aorta from 4D flow MRI using deep learning," *Magn. Reson. Imag.*, vol. 99, pp. 20–25, Jun. 2023.

[100] A. Jafar, M. T. Hameed, N. Akram, U. Waqas, H. S. Kim, and R. A. Naqvi, "CardioNet: Automatic semantic segmentation to calculate the cardiothoracic ratio for cardiomegaly and other chest diseases," *J. Personalized Med.*, vol. 12, no. 6, p. 988, Jun. 2022.

[101] K. Giannakaki, K. Moirogiorgou, M. Zervakis, N. Anousakis-Vlachochristou, G. K. Matsopoulos, C. Komporozos, V. Sourides, G. Katsimagklis, M. Drakopoulou, K. Toutouzas, C. Avgeropoulou, and A. Androulakis, "Automatic aortic valve area detection in echocardiography images using convolutional neural networks and U-net architecture for bicuspid aortic valve recognition," in *Proc. IEEE Int. Conf. Imag. Syst. Techn. (IST)*, Aug. 2021, pp. 1–6.

[102] T. Park, S. Khang, H. Jeong, K. Koo, J. Lee, J. Shin, and H. C. Kang, "Deep learning segmentation in 2D X-ray images and non-rigid registration in multi-modality images of coronary arteries," *Diagnostics*, vol. 12, no. 4, p. 778, Mar. 2022.

[103] K. W. Lai, M. A. Shoaib, J. H. Chuah, M. H. A. Nizar, S. Anis, and S. L. W. Ching, "Aortic valve segmentation using deep learning," in *Proc. IEEE-EMBS Conf. Biomed. Eng. Sci. (IECBES)*, Mar. 2021, pp. 528–532.

[104] S. Nurmaini, M. N. Rachmatullah, A. I. Sapitri, A. Darmawahyuni, B. Tutuko, F. Firdaus, R. U. Partan, and N. Bernolian, "Deep learning-based computer-aided fetal echocardiography: Application to heart standard view segmentation for congenital heart defects detection," *Sensors*, vol. 21, no. 23, p. 8007, Nov. 2021.

[105] S. Kang, S. J. Kim, H. G. Ahn, K.-C. Cha, and S. Yang, "Left ventricle segmentation in transesophageal echocardiography images using a deep neural network," *PLoS One*, vol. 18, no. 1, Jan. 2023, Art. no. e0280485.

[106] R. Elshawi, A. Wahab, A. Barnawi, and S. Sakr, "DLBench: A comprehensive experimental evaluation of deep learning frameworks," *Cluster Comput.*, vol. 24, no. 3, pp. 2017–2038, Sep. 2021.

[107] C. Sudlow, J. Gallacher, N. Allen, V. Beral, P. Burton, J. Danesh, P. Downey, P. Elliott, J. Green, M. Landray, B. Liu, P. Matthews, G. Ong, J. Pell, A. Silman, A. Young, T. Sprosen, T. Peakman, and R. Collins, "UK Biobank: An open access resource for identifying the causes of a wide range of complex diseases of middle and old age," *PLOS Med.*, vol. 12, no. 3, Mar. 2015, Art. no. e1001779.

[108] R. Girdhar, A. El-Nouby, Z. Liu, M. Singh, K. V. Alwala, A. Joulin, and I. Misra, "ImageBind one embedding space to bind them all," in *Proc. IEEE/CVF Conf. Comput. Vis. Pattern Recognit. (CVPR)*, Jun. 2023, pp. 15180–15190.

TALHA IQBAL received the Ph.D. degree from the University of Galway, Galway, Ireland, in 2023. He is currently pursuing the Postdoctoral degree with the Insight SFI Research Center for Data Analytics, University of Galway, Ireland. His current research interests include the disciplines of engineering and medicine, with a focus on AI/machine learning, data science, biosensors, wearable devices, and signal processing. He was a recipient of the COMSATS Full-Time Scholarship (A+ category), from 2017 to 2018; the QCRI/Boeing Travel Grant, Qatar, in 2018; the Top-10 APPRC Award Australia, from 2017 to 2018; and the Scholarship under SFI Professorship Award, Ireland, in 2019.

OSAMA SOLIMAN is currently a clinical cardiologist with more than two decades of experience in cardiovascular imaging, clinical trials, and innovation in medicine, and has pioneered several non-invasive imaging techniques and methods. He holds the position of Professor with a Personal Chair in cardiovascular research with the University of Galway, Galway, Ireland. He is also the Co-Founder and the Medical Director of the CORRIB Research Center for Advanced Cardiovascular Imaging and Core Laboratory, which is a research laboratory for precision medicine. In addition, he is the Director of the Cardio-Oncology Research Program, CORRIB Research Center for Advanced Cardiovascular Imaging and Core Laboratory. He is a regular Faculty at several top Cardiology and Cardiothoracic Surgical Conferences, including the annual meetings of the ESC, EACTS, ACC, TCT, EuroPCR, EuroEcho, and PCR-London Valves. His current research interests include the application of precision medicine in the management of patients with heart failure and guiding structural heart interventions.

SHERIF SULTAN is currently the Clinical Vascular Lead with the Soalta Hospital Group, National Health Service Executive. He heads a team of dedicated vascular and endovascular specialists, with a focus on the prevention of cardiovascular morbidity and mortality. He specializes in stroke prevention with one-day surgery for carotid artery intervention; and endovascular, open, and hybrid management of thoracic and abdominal aortic aneurysm and dissection. In addition, he performs keyhole surgery for varicose veins as a 6-h outpatient admission. With state-of-the-art technology, vascular laboratory, veins unit, diagnostic and interventional capabilities, comprehensive research programs, and ongoing educational opportunities, he delivers the highest level of care to meet the needs of his vascular patients. He established the first vascular genetic clinic in Ireland and initiated the program of buccal genetic screening for vascular connective tissue disorders.

IHSAN ULLAH received the Ph.D. degree from the University of Milan, Italy, in 2017. Currently, he is an Assistant Professor with the School of Computer Science, University of Galway, Ireland. He is a Principal Investigator of the SFI Funded National Challenge Fund Project and a Funded Investigator of the Insight SFI Research Center for Data Analytics, Galway. His current research interests include mainly designing lightweight neural networks, federated learning, image/video processing, medical image analysis, signal processing, deep learning, and explainable AI.